THE ELECTRONIC PROPERTIES
OF METAL SOLUTIONS IN LIQUID AMMONIA
AND RELATED SOLVENTS

PETER P. EDWARDS

University Chemical Laboratory, Cambridge, England

I. Introduction

The introduction of sodium metal into anhydrous liquid ammonia produces an intensely colored blue solution in which solvated electrons, sodium cations, and various agglomerates of these species coexist in equilibrium. With increasing metal concentration, the system transforms into a bronze-colored metallic conductor with an equivalent conductance exceeding that of liquid mercury. In the transitional range, cooling of the homogeneous solution can give rise to a remarkable liquid–liquid phase separation in which both dilute (blue) and concentrated (bronze) phases coexist. The underlying experimental simplicity of this system, which exhibits the localization of the fundamental unit of electrical charge in dilute solutions and its itineracy in concentrated solutions, has attracted a considerable amount of study from both chemists and physicists for over a century (*37–39, 99, 103, 113, 116, 164, 172*).
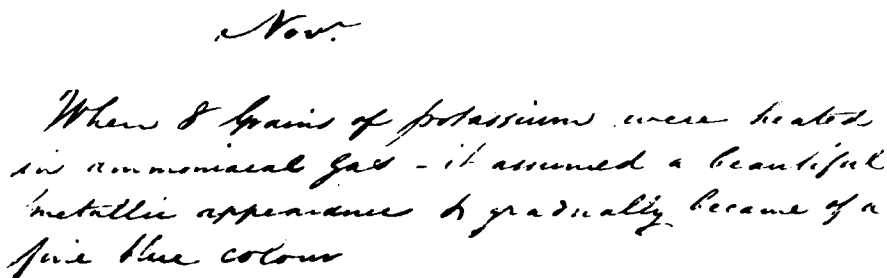
Although we routinely attribute the discovery of metal–ammonia solutions to the German chemist Weyl in 1863 (*172*), they were proba-

bly first prepared over 50 years earlier by Sir Humphry Davy. Following his discovery and isolation of potassium and sodium in October 1807 (46), Davy conducted a long series of experiments on the reaction between potassium and gaseous ammonia to support his contention that potassium was indeed an element and not a hydride of potash, as suggested by Gay-Lussac and Thenard (136). Throughout this investigation, Davy had consistently stressed (136) the overriding importance of working with dry ammonia, a precaution apparently neglected by the French chemists of the day. An entry (Fig. 1) by Davy for November 14 (or thereabouts) 1808 in his experimental notebook is one of many referring to numerous experiments conducted on the mutual action of potassium and ammonia with each other:

> When 8 grains of potassium are heated in ammoniacal gas—it assumed a beautiful metallic appearance & gradually became of a fine blue colour . . .

Several other entries in this period refer to similar observations. As far as I am aware at the present time, these observations were never published in the scientific literature (79), although Davy in the same notebook does make some remarkably perceptive comments regarding these systems (Section V).

The physical properties of these intriguing systems have been studied in serious vein since the 1920s (111, 164). At the present time, this interest continues unabated. In its more recent development, the multidisciplinary nature of metal-solution investigations has also spilled over into the wider fields of excess electrons in disordered media (38, 39, 99, 103). The recent Colloque Weyl V conference on metal-ammonia solutions and excess electrons in liquids (39) brought together almost 200 scientists from all disciplines. The present review

FIG. 1. An entry from the laboratory notebook of Sir Humphry Davy for the period October 1805–October 1812. The entry is for November 1808; a more precise location is rather difficult, but various entries around the same period suggest November 14 as the most likely date. Reproduced by courtesy of the Royal Institution, London, England.

attempts to cover the electronic properties of metal solutions in the dilute and concentrated ranges, as well as a cursory examination of the nature of the nonmetal-to-metal transition in these systems. In a review some 45 pages long one cannot expect to do justice to the sheer depth and extent of investigation into these systems. In particular, metal–ammonia solutions must be one of only a few systems (if not *the* only one) that can boast reliable and comprehensive optical, conductivity, and magnetic data (among other properties) over something like five orders of magnitude in concentration (*37, 164*).

My aim here is to provide a general background discussion centered around recent advances in studies of metals, not only in ammonia but also in various other solvents. To this author, one of the most important features to emerge from investigations into metal solutions over the last two decades has been the striking advances made possible from studies of metals in nonaqueous solvents other than ammonia. As Dye has suggested (*55*), in any description of metal solutions, we invariably return to the ammonia system for guidance. Certainly in this solvent we have, at the present time, the most data on physical and chemical properties (*164*). In this spirit, the electronic properties of dilute, intermediate, and concentrated metal–ammonia solutions form the underlying framework for this review, and these are discussed at various points in Sections II–IV.

However, in contrast to the ammonia system, metal solutions in amines, ethers, and related solvents are rich in information about *distinguishable* species existing in dilute solutions (*53, 55*). Sections II and III,B will similarly outline certain recent developments in these solvent systems, which have led to a fairly detailed picture of localized-electron states in the dilute range.

Section IV gives an overall view of concentrated solutions and the nonmetal–metal (NM-M) transition. Here again, the majority of data are for metal–ammonia solutions. However, in the past decade a substantial body of experimental data has emerged for the NM-M transition in lithium–methylamine solutions, which allows a direct comparison with the situation existing in metal–ammonia solutions (*60*). This section also considers recent developments in the study of the "expanded-metal" compounds, as typified by $Li(NH_3)_4$, $Ca(NH_3)_6$ (*82*), and $Li(CH_3NH_2)_4$ (*66*), and formed by slow cooling of the concentrated metal solutions.

Throughout this review, metal concentrations are expressed in units of mole percent metal (MPM), where

$$\text{mole percent metal} = \left| \frac{\text{moles metal}}{(\text{moles metal} + \text{moles solvent})} \right| \times 100$$

II. The Isolated Solvated Electron in Dilute Solutions

The accumulated evidence for the electrolytic nature of dilute metal solutions is overwhelming—metal atoms introduced into a variety of nonaqueous solvents spontaneously dissociate into localized excess electrons and positive ions (*37, 39, 164*).

$$Na \rightarrow Na^+ + e^- \tag{1}$$

We recall that the corresponding process (*22*) in the *gas phase* requires an energy of $\sim 2-4$ eV! Drawing upon the analogous situation in "conventional" electrolyte systems, e.g., aqueous salt solutions, one infers that both species are "solvated" in the sense that they polarize the surrounding dipolar solvent molecules in their own Coulombic field (*101, 104*). The idea of solvating a fundamental particle is indeed intriguing. Kraus (*109–111*) first proposed that the excess electron existed in a cavity in the solvent in which one or more of the ammonia molecules have been excluded, thereby accounting for the extremely low density of the solutions (*37*). However, it was Gibson and Argo (*80*) who were the first to apply the description "solvated electron," e_s^-, for the excess electron states in liquid ammonia.†

In the period 1940–1946, Ogg (*132*) developed the first quantitative theory for the solvated electron states in liquid ammonia. The Ogg description relied primarily on the picture of a particle in a box. A spherical cavity of radius R is assumed around the electron, and the ammonia molecules create an effective spherical potential well with an infinitely high repulsive barrier to the electron. It is this latter feature that does not satisfactorily represent the relatively weakly bound states of the excess electron (*9, 103*). However, the idea of a potential cavity formed the basis of subsequent theoretical treatments. Indeed, as Brodsky and Tsarevsky (*9*) have recently pointed out, the simple approach used by Ogg for the excess electron in ammonia forms the basis of the modern theory (*157*) of localized excess-electron states in the nonpolar, rare-gas systems. [The similarities between the current treatments of trapped H atoms and excess electrons in the rare-gas solids has also recently been reviewed by Edwards (*59*).]

Jortner, in a milestone contribution (*101, 104*), elaborated on this

† The short-lived hydrated electron counterpart, e_{aq}^-, was discovered in the early 1960s in water and in aqueous electrolyte solutions (*7, 90*). These hydrated electrons have since been found to play an important role in radiation-induced chemical conversions and in the changes in the physical properties of irradiated aqueous systems (*39, 140*). Solvated electrons have also been observed in a variety of nonpolar (*45*) as well as polar liquids. For a recent review, see Kevan and Feng (*74*).

simple physical picture. He supposed that the electron resided in a cavity of radius R approximately 3.2–3.4 Å in the ammonia. The liquid ammonia in the vicinity of the cavity is polarized by the electron, producing a centrally symmetric potential well of the type

$$V_{(r)} = \begin{cases} \dfrac{-e^2}{\epsilon_{\text{eff}}R} & r < R \\[2mm] \dfrac{-e^2}{\epsilon_{\text{eff}}r} & r \geq R \end{cases} \quad \epsilon_{\text{eff}}^{-1} = \epsilon_\infty^{-1} - \epsilon_0^{-1}$$

(2)

(3)

where ϵ_∞ and ϵ_0 are the high- and low-frequency dielectric constants, respectively. Thus the model combines the idea of Ogg's cavity with a polarization interaction at large distances.

Following a variational solution of the ground (1s) and first excited state (2p) of the electron in this potential well, various other polarization terms are added and a variety of characteristics for the solvated electron (optical transition energy, heat of solution, etc.) can be calculated (101, 105). For illustrative purposes, we shall utilize this simple model because of its obvious transparency in relating certain (macroscopic) features of solvent properties to the energy levels and wave functions for the solvated electron in polar solvents.

The derived potentials, energy levels, and wave functions for the solvated electron in two representative solvents, methylamine and hexamethylphosphoramide (HMPA), are compared in Fig. 2. A characteristic broad optical-absorption band in the near infrared (see Fig. 12, Section III,B,2 for a typical trace) is generally attributed (101, 104) to the Franck–Condon 1s → 2p transition within this potential well. Theory predicts (9, 104, 146, 147) and experiments confirm (146, 152) a high transition probability for this excitation, giving rise to the intense blue color characteristic of these systems. On this model, the solvent is considered only in terms of a continuum for $r > R$, and no account is taken of the peculiarities of the local structure around e⁻—for example, in the first coordination layer of the cavity (105). On a simplified approach, the energy of the optical transition energy might be judged to be coarsely related to the binding energy of the solvated electron in that solvent. However, the exact nature of electron binding and the associated lifetime of the solvated entity in polar solvents is a complex problem (1, 102, 105, 120, 171). Lifetime considerations (146) also have to take into account the pseudobimolecular reaction of electrons in the solvent, e.g., in water,

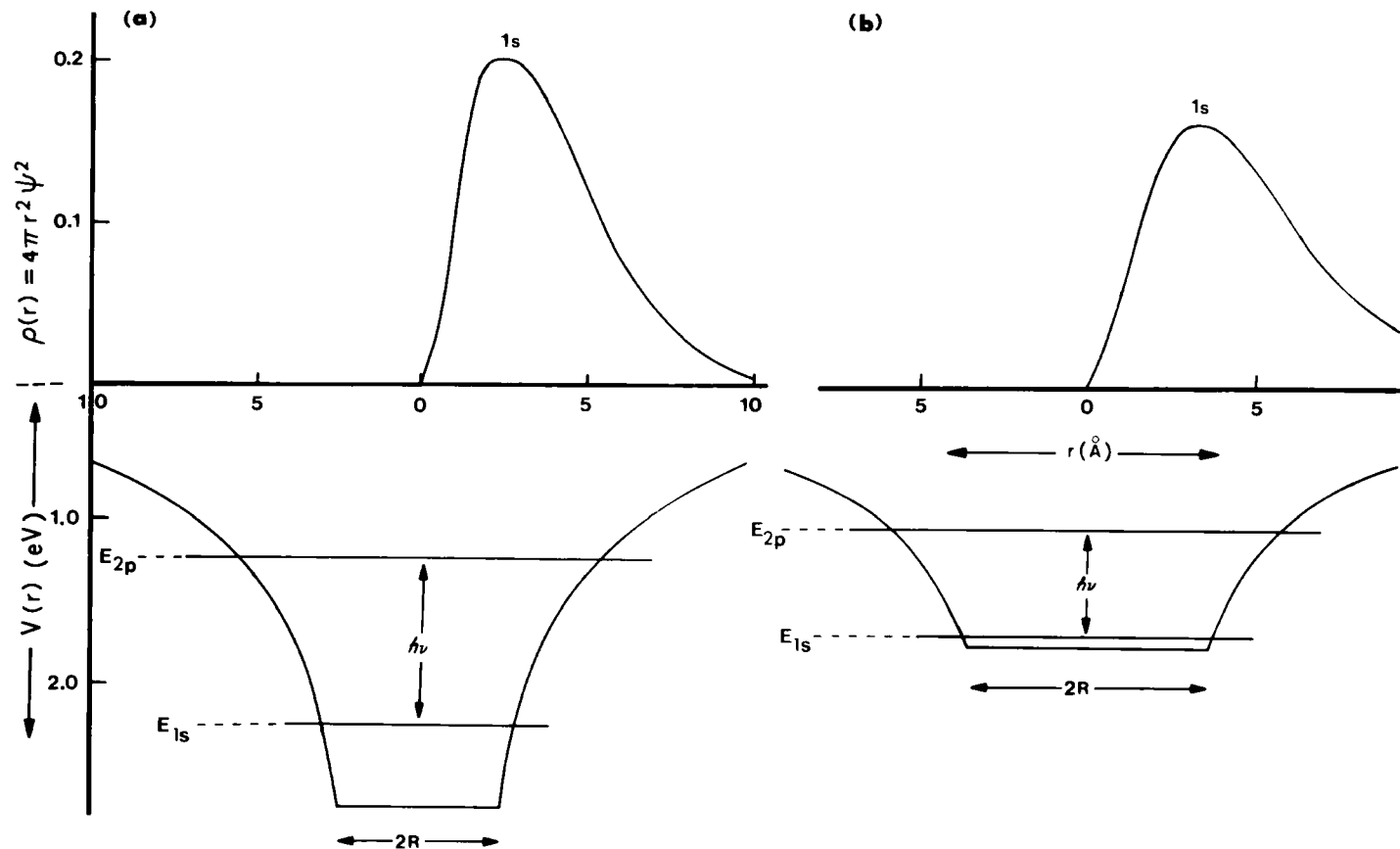$$2e_{\text{aq}}^- + 2H_2O \rightarrow H_2 + 2OH^-$$
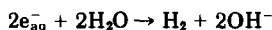
FIG. 2. Wave functions and energy levels for the solvated electron in (a) methylamine (MeA) and (b) hexamethylphosphoramide (HMPA). The potential $V(r)$ and wavefunction are based upon the model of Jortner (101) and computed using values of the optical and static dielectric constants of the two solvents. The optical absorption responsible for the characteristic blue color is marked by $h\nu$ and represents transitions between the 1s and 2p states. The radius of the cavity is ~3 Å in MeA, and ~4.5 Å in HMPA.

(pseudobimolecular rate constant $k = 5 \times 10^9$ liter mol^{-1} sec^{-1}). The relative stability of the spin-paired dimer species in ammonia (Section III,A,2) may well retard the corresponding reaction of electrons in this solvent (54, 146).

For our illustrative purposes, HMPA is taken as representative of a large, bulky, aprotic solvent in which electron and, indeed, any anion solvation is very weak (129, 131). Methylamine is representative of a solvent in which the electron binding is considerably larger (60, 127). Within the cavity, the electronic wave function assumes its maximum value; outside the cavity, the wave function asympotically approaches zero. Although there is obviously a high degree of charge confinement within the cavity, a considerable amount of charge dispersion exists far beyond the first solvation layer.

All attempts (74, 89) to find a sensible, quantitative relation between the wavelength of maximum absorption (λ_{max}) and typical macroscopic properties of the solvent (i.e., dielectric constant) have so far failed (146). However, the size of the solvent cavity in which the electron is trapped also plays a decisive role (101) in determining the transition energy [Eqs. (2), (3)], and the solvent dependence of λ_{max} might well indicate a variation in cavity size from solvent to solvent. In this spirit, Dorfman and Jou (48) have evaluated cavity radii on the basis of the simple Jortner model for the solvated electron. The values are shown in Fig. 3, which shows a plot of the optical transition energy E_{max} versus
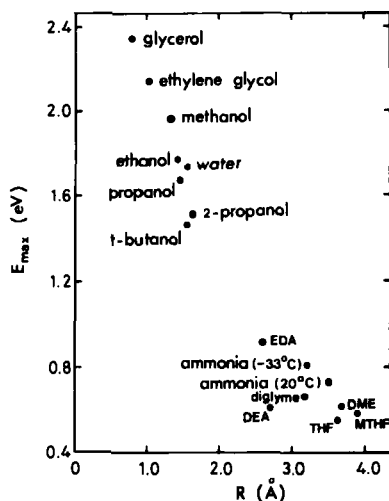

FIG. 3. Values of the cavity radius R calculated, from Jortner (101), to fit the values for E_{max}. [From Dorfman and Jou (48), Fig. 9. Reprinted with permission from Springer-Verlag, Berlin.]

R. The cavity radii in water and alcohol are around 0.9–1.5 A, and in ammonia and the various amines and ethers between 2.5 and 4 Å.

Considerably more elaborate treatments (*1, 40, 105*) for calculating the electronic energy levels and wave functions for the excess electron have since been developed and attempt to introduce certain microscopic features of the local molecular environment. Such calculations for electrons in ammonia were first reported by Copeland, Kestner, and Jortner (*40*). The reader is referred to the paper by Banerjee and Simons (*1*) and the recent review by Brodsky and Tsarevsky (*9*) for comprehensive discussions of the current theoretical descriptions for solvated electrons in disordered condensed media (see also Ref. *171*).

III. Electronic Properties of Dilute Solutions

Numerous physical and chemical investigations (*37–39, 99, 103, 113, 116, 164*) of metals in nonaqueous solvents reveal unequivocally that solvated electrons and metal cations interact in the dilute and intermediate concentration range to form various agglomerate species, both paramagnetic and diamagnetic. In this section we attempt to illustrate the rich variety of these localized-electron species in dilute solutions. We begin with a short summary of the situation in metal–ammonia solutions. Our objective here is twofold: (1) to set the scene for our later discussions concerning the transition to the metallic state in more concentrated metal solutions, and (2) to allow a comparison of the situation existing in dilute ammonia solutions to that found in the lower-dielectric-constant amine and ether solvents.

A. METALS IN LIQUID AMMONIA

The overall changes in magnetic and transport properties of metal–ammonia solutions from the dilute to concentrated regimes are shown in Fig. 4.

1. Electron–Cation Interactions

As with any electrolyte, various aggregate species are expected to form as the concentration of solute increases. In particular, both the electrical conductivity and (metal) NMR data (Fig. 4) signal the appearance of neutral species at metal concentrations in excess of 10^{-3} MPM (*37*), the conductivity via a Morse-like behavior in the equivalent conductance, the magnetic resonance via a finite Knight (contact) shift

for the metal nucleus. As expected for a high-dielectric-constant solvent, the ion-pairing association

$$M_s^+ + e_s^- \leftrightharpoons (M_s^+, e_s^-) \tag{4}$$

is best viewed as a simple (and very short-lived (26), ~10^{-12} sec) ionic aggregation involving a complex in which there is negligible distortion of either the solvated electron or solvated cation wave function. The very small electron spin density at the metal nucleus [judged from the metal Knight shift (13) data to be approximately 1% of the free-atom value] does indeed indicate a weakly interacting association complex (54). In the concentration range where the ion-pairing process is quite clearly indicated by the conductivity and NMR data, the optical absorption peak shows certain minor but significant modifications (Fig. 4). The observed red shift of this band [for a recent compilation of data, see Harris (88)] with solution composition in the range 10^{-3} to 10^{-1}
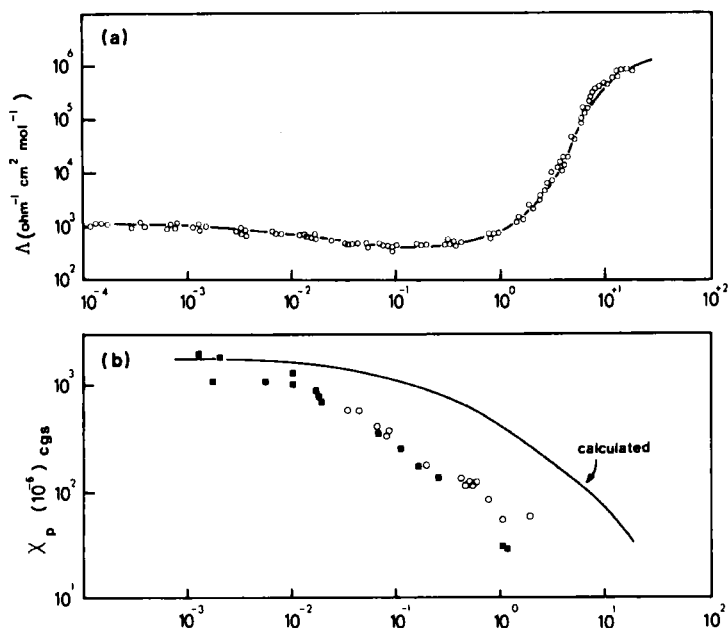

FIG. 4. The concentration dependence of various electronic properties of metal-ammonia solutions. (a) The ratio of electrical conductivity to the concentration of metal-equivalent conductance, as a function of metal concentration (240 K). [Data from Kraus (111).] (b) The molar spin (O) and static (■) susceptibilities of sodium–ammonia solutions at 240 K. Data of Hutchison and Pastor (spin, Ref. 98) and Huster (static, Ref. 97), as given in Cohen and Thompson (37). The spin susceptibility is calculated at 240 K for an assembly of noninteracting electrons, including degeneracy when required (37).
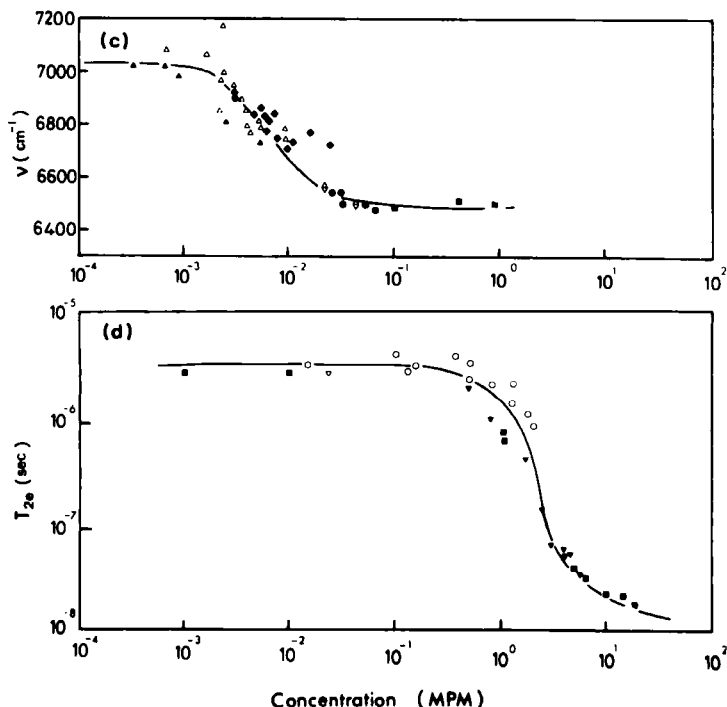
FIG. 4. (continued) (c) The optical properties of sodium–ammonia and potassium–ammonia solutions (208 K), and variation of the near-IR band maxima with concentration. [Data of Douthit and Dye (49), Gold and Jolly (84), Koehler and Lagowski (107), Rubinstein et al.(144), and Quinn and Lagowski (142), as given by Harris (88).] (d) ESR spin–spin relaxation time T_{2e} at 238 K. [Data from Chan et al. (∇, Ref. 31), Essig ($\blacksquare$, Ref. 72), and Hutchison and Pastor (O, Ref. 98), as given in Schindewolf (148).]

MPM ($-65°C$, 208 K) was originally attributed (49) to ion-pair formation [Eq. (4)]. However, more recent work (144) suggests the shift results from the presence of two absorption centers in the intermediate concentration range: the solvated electron and a second absorber involving a binary combination of solvated electrons, a diamagnetic species. The precise origins of this red shift in the optical band in ammonia solutions are still a matter of some controversy. However, the accumulated evidence for the link between the *red* shift and *electron spin-pairing* is extremely strong (144, 165). In addition, recent precise studies of optical band shapes for the solvated electron in ethylenediamine (see Section III,B,2) suggest a *blue* shift upon *ion-pairing* (150), as observed for the (M_s^+, e_s^-) species in a variety of solvent systems (65, 151, 153).

Another important property, the apparent molar volume of the solvated electron, is essentially unaffected by the electron–cation and, indeed, the electron–electron interaction (*37*).

In summary then, the appellation (*53, 84, 85*) "loose ion-pair" for the solvated electron–metal cation association complex in dilute metal–ammonia solutions is therefore a particularly apt description.

2. Electron–Electron Interactions

The nature of the interaction leading to electron *spin-pairing* is far less clear (*54*). The rapid decrease in the molar spin susceptibility of metal–ammonia solutions in the concentration range 10^{-3} to 1 MPM below that expected for an assembly of noninteracting electrons (Fig. 4) has been taken as direct evidence for the formation of diamagnetic complexes having an even number of electrons in a singlet ground state (*37, 54*). For example, at 0.1 MPM, approximately 90% of the electrons in a sodium–ammonia solution are spin-paired, and the diamagnetic state is apparently several times kT (thermal energy) lower in energy than the triplet or dissociated doublet states. In addition, lower temperatures favor the diamagnetic state. Figure 5 shows the experimental data for metal ammonia solutions at 25°C (298 K), 0°C (273 K), and −33°C (240 K), expressed in terms of paramagnetic spin concentrations (*88*).

In the weak-interaction model (*85*) developed in the previous section to explain ion-pairing in metal–ammonia solutions, aggregation interactions involving M_s^+ and e_s^- are relatively weak, and leave the isolated solvated electron properties virtually intact. However, a major difficulty (*29, 54, 134*) arises with the type of model when one considers the precise nature of the corresponding electron spin-pairing interaction in ammonia solutions. It is worth expanding on this issue because it probably remains one of the fundamental dilemmas of metal–ammonia solutions in the dilute range (*54*).

The mere existence of diamagnetic states in dilute metal–ammonia solutions in itself presents no direct threat to a weak-interaction model; spin–spin interactions could presumably be incorporated into an ion-cluster model (*85*), where spin pairing occurs via collision complexes or by a long-range interaction between isolated solvated electrons, possibly mediated via an intermediate cation. In a recent study of solvated electron interactions, Schettler and Lepoutre (*145*) found that the ground singlet state is separated from the lowest triplet state by kT at interunit separations below 10.5 Å. However, we note that the mean distance between metal atoms in the spin-pairing concentration range
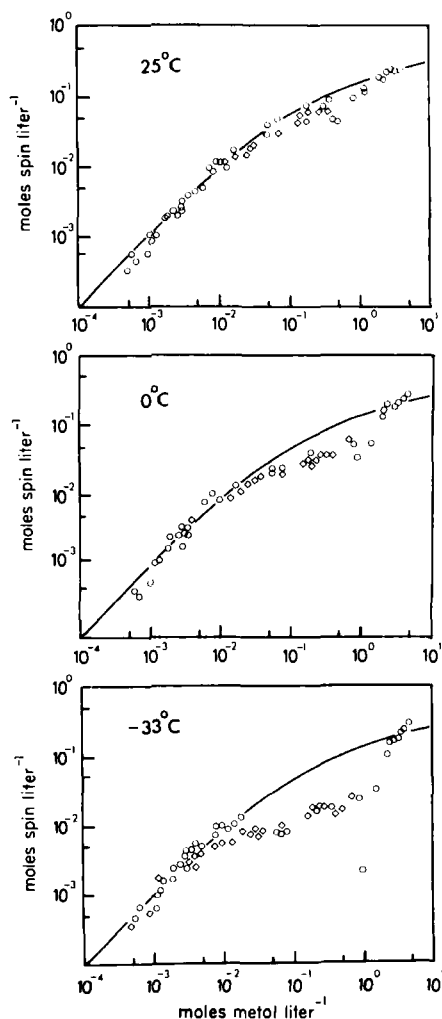
FIG. 5. Electron spin pairing in metal–ammonia solutions at 25°C (298 K), 0°C (273 K), and −33°C (240 K). Paramagnetic spin concentrations for sodium–ammonia and potassium–ammonia solutions. [Experimental data from Refs. *47, 76, 98, 114, 115,* and *159.* Adapted from Harris (*88*). Used with permission.] The solid line indicates the expected spin-pairing behavior for noninteracting electrons (*88*).
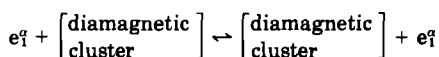
(10^{-3} to 10^{-2} MPM) is ~90 to 180 Å! The long-range interaction picture runs into an even more fundamental difficulty when one considers the exceptionally long lifetime (~1 μsec) of the electron–electron spin-pairing interaction required to maintain the electron spin-state lifetimes, as detected by ESR (*134*). Measured electron spin–spin relax-

ation times (T_{2e}) for solutions in the concentration range 10^{-4} to 10 MPM are shown in Fig. 4d. These ESR linewidths (ΔH) are among the narrowest known (typically in the region 0.02 to 0.03 G) and, particularly for the lighter alkali metals (134), are essentially constant over the composition range in which extensive spin pairing is taking place (37). In the light of the above comments concerning solvated electron interactions, a long-range interaction between solvated electrons in the concentration range 10^{-3} to 10^{-2} MPM might be expected to produce relatively weakly bound diamagnetic units, which would rapidly separate into two individual e_s^- units. This should lead to a considerable uncertainty in the electron spin lifetime and *an electron spin relaxation rate that is markedly composition dependent*. This effect is *not* observed (Fig. 4). The extremely narrow ESR, with its attendant long T_{2e} $(T_{2e} \approx 1/\Delta H)$ in the μsec range (29, 134), then requires (54) that processes of the type

$$e_1 + e_1 \rightleftharpoons e_2 \tag{5}$$
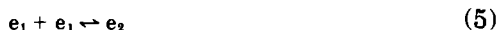
have encounter lifetimes *exceeding* 10^{-6} sec (recall that the corresponding lifetime of electron–cation encounter ion pairs in dilute ammonia solutions is only $\sim 10^{-12}$ sec). Thus the singlet state, once formed, must apparently exist for a microsecond or longer before conversion into a dissociated pair of electrons.

It has been suggested (54) that the exceptionally long lifetime of the singlet e_2 state may still arise from weak, long-range interactions, but with the stringent lifetime requirements being satisfied through additional electron-exchange processes of the type

$$e_1^q + \begin{bmatrix} \text{diamagnetic} \\ \text{cluster} \end{bmatrix} \rightleftharpoons \begin{bmatrix} \text{diamagnetic} \\ \text{cluster} \end{bmatrix} + e_1^q$$

However, this scheme does present major conceptual difficulties and has been criticized recently (160). In particular, the formation of specific diamagnetic (cluster) units at these very low metal concentrations might be considered unrealistic in view of the extremely large (average) electron–electron separation (~ 100 Å). Clustering phenomena are well established for concentrations close to the nonmetal-to-metal transition in these systems (33, 155), but for sodium–ammonia solutions this does not occur until approximately 4 MPM (Section IV).

Even without the complexities introduced via electron-exchange processes of the type outlined above, the fundamental nature of the interaction between two solvated electrons leading to spin pairing has yet to be firmly established. A treatment of the possible bonding in

terms of a valence bond approximation has been attempted by Schettler and Lepoutre (145), stressing the diffuse nature (Fig. 2) of the trapping potential for the solvated electron. This treatment takes no account of the (rapidly) varying electron density with metal composition. A super-exchange-type process, involving an intermediary metal cation, is implicit in the recent suggestion of Mott (122) for the spin-paired species in ammonia. While there is some evidence for "ion triples," $e_s^- M_s^+ e_s^-$, in a recent study of lanthanoid metals in ammonia (138), the suggestion has also come under some criticism (14). Clearly, charge neutrality *might* demand (133) some cation involvement, but the details of the interaction remain to be firmly established.

Two final points are of interest. First, in the overall context of spin pairing in dilute solutions, and the subsequent "metallization" process at higher concentrations [Fig. 4(a)], it is important to note that as the system moves *through* the nonmetal-to-metal transition (located around 4 MPM), the paramagnetic susceptibility quite rapidly approaches the predicted value for an assembly of degenerate (metallic) electronic states (37) (see also Fig. 5). The possible implications of this observation to the nature of spin pairing in the nonmetallic regime are discussed by Edwards (62). Second, the concept of *null properties* in dilute metal–ammonia solutions—i.e., properties which are essentially insensitive to metal concentration—formed the observational basis (54) for the weak-interaction (85), ion-cluster model (Section III,A,1). In this, complexes are formed from individual units which retain their essential properties in the loosely bound agglomerate species. However, it is amusing to note that the insensitivity of T_{2e} to metal concentration in the dilute regime (Fig. 4) now forms the observational basis for a model that demands a *stable, long-lived* diamagnetic entity in dilute metal–ammonia solutions (54).

The time is indeed ripe for more detailed experimental and theoretical studies of the spin-pairing phenomenon in metal solutions. Indeed, a considerable portion of the experimental data in this controversial area dates back to the late 1950s, and, for some data, even earlier (76).

B. METALS IN AMINES, ETHERS, AND OTHER SOLVENTS

One underlying theme to emerge from the previous section is the lack of specific information regarding *distinguishable* species in dilute metal–ammonia solutions (55). This might well be anticipated to be a natural consequence for agglomerate species in a host solvent with a large dielectric constant ($\epsilon_0 = 16$ at 300 K). In general terms, the prop-

erties of dilute metal–ammonia solutions are then best characterized
(22) in terms of an assembly of isolated fragments (M_s^+, e_s^-) in which the
excess-electron state forfeits any parentage in the electronic states of
the gas-phase alkali atom.

In contrast to ammonia solutions, in which the metal cation effec-
tively assumes a "bystander" role in the formation of aggregate species,
metal solutions in the low-dielectric-constant amines and ethers (ϵ_0
typically <10 at 300 K) show a multitude of metal-dependent species,
both paramagnetic and diamagnetic. The general body of experimental
information requires the presence of at least *three distinct stoichiome-
tries* in solution (51, 53, 55),

$$M_s^+ + e_s^- \leftrightarrow (M_s^+, e_s^-) \leftrightarrow (M_s^-), \tag{6}$$
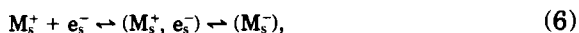
the solvated electron, an aggregate species of e_s^- and M_s^+, and a dielec-
tron species, now well characterized in certain solvents (51, 52) as a
centrosymmetric (solvated) alkali metal anion (M_s^-). The association of
(solvated) cation and electron can no longer be described as a weakly
interacting ion-pair species; in these solvents we have immediately
recognizable changes in the electronic properties of the aggregate
species compared to its constituent partners. A problem of classifica-
tion now enters (51, 53) when, for example, terms such as "loose" and
"contact" ion pairs and "monomers" are introduced to describe the as-
sociation complex (143). It is to this problem that we turn to in the
following section. However, at this stage we may safely make the gen-
eral comment that the majority of aggregate species are more "tightly
bound" than in ammonia solutions—as indeed one would expect from
the decrease in dielectric constant. By this we mean that the
electron–cation interaction can be sufficiently strong to introduce a
noticeable metal dependence into the electronic properties.

This metal dependence also carries over to the spin-paired species. In
the low-dielectric-constant solvents, these can no longer be represented
in terms of weak, long-range interactions possibly mediated by an in-
tervening cation, but are now distinct, new molecular entities (Section
III,B,5).

In most general terms, the species identified in metal solutions are
best described as "matrix-bound," in that the system comprises a solute
(metal) species in a host (solvent) matrix. Before discussing details of
the experimental data, we first attempt a general rationalization (61,
108) of the spectrum of possible matrix-bound states found in metal
solutions.

1. Paramagnetic States: Ion Pairs to Solvated Alkali Metal Atoms

Consider the incorporation of a rubidium atom into a polar solvent and imagine that the valence (5s) electron is removed from it, leaving behind a positive ion Rb^+. This ion will polarize the surrounding solvent so that at *large distances* it produces an electrostatic potential (*108*)

$$U = (e/\epsilon_0)r \qquad (7)$$

where ϵ_0 is the static dielectric constant. When (and if) the valence electron is brought back, one of several situations may result (*106, 170*).

(i)   It may be energetically favorable for the valence electron to occupy a large centrosymmetric orbit, over most of which Eq. (7) applies. The Coulombic attraction between the positive hole and the bound electron is reduced by the static dielectric constant of the solvent. The solute ion–solvent interaction effectively reduces or screens the Rb^+–valence electron interaction. In terms of a centrosymmetric picture (*3, 4*) for a monomer species (see Fig. 6), this results in a substantial increase in the Bohr radius† (a_H^*) of the 5s-electron wave function. In this situation, the potential is basically Coulombic, and the matrix-bound states are closely related to the corresponding states of the hydrogen atom,‡ i.e., via a modified Schroedinger equation (*5, 108*) in which the potential is given by Eq. (7) and the modified Bohr radius by

$$a_H^* = (\epsilon_0)a_0/m^* \qquad (8)$$

where m^* is an effective mass for the excess electron, and a_0 is the Bohr radius of the hydrogen 1s orbital (0.5292 Å). It is important to note that in the limiting situation, matrix-bound states characterized by this screened hydrogenic potential [Eq. (7)], although spatially localized around the Rb^+ core, have *no* recognizable characteristics of the gas-phase Rb atom (*5, 106, 108, 170*). Eigenfunctions and eigenenergies are *solely* dependent upon the characteristics (m^*, ϵ_0) of the host solvent. As such it would be very difficult to differentiate their electronic properties from those of the *isolated* excess electron [see also (iv)]. Such states

---

† Approximately taken as the radius of maximum spin density $(4\pi r^2\psi^2)$ of the valence electron.

‡ The related situation in highly excited states of the alkali atoms has recently been reviewed by Metcalf (*121*).
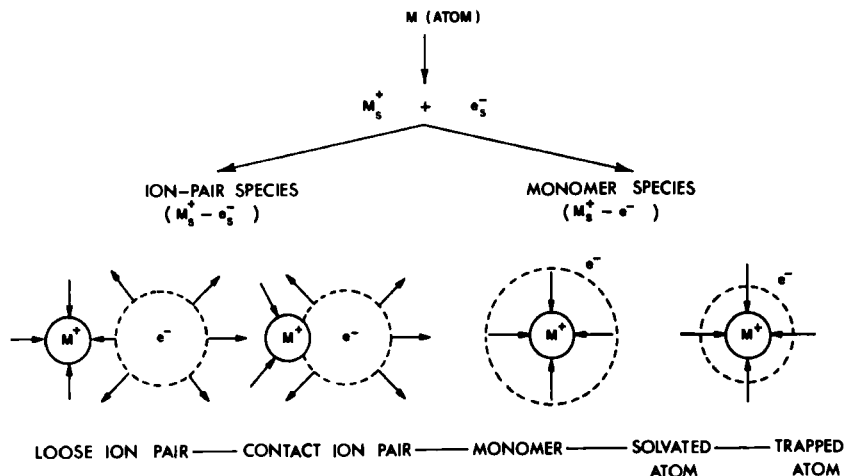
FIG. 6. A schematic representation of several possible (paramagnetic) electron–cation aggregates in metal solutions. [Adapted from Fig. 3 of J. L. Dye (53), with permission from Pergammon Press.]

have indeed been identified (18) in frozen solutions of alkali metals in HMPA (Section III,B,4). An alternative, pictorial representation of this type of weakly interacting state is the "loose" ion-pair species (53), and is also shown in Fig. 6. This latter type of representation emphasizes directional bonding between the constituent partners. We note that in the absence of this directional interaction, there is essentially no distinction between this representation and the large radius monomer state. This aspect is discussed elsewhere (61).

(ii)   The most favorable energy state for the electron may be to occupy an orbit very near to the rubidium cation. In this case, Eq. (7) does not apply and we have the possibility of a complicated state of affairs in the immediate vicinity of the cation (108). If there exists only a weak pertubation by the surrounding matrix (170) (for example, in the rare-gas solids), we have a "trapped atom" situation (Fig. 6). These states are adequately described (100) in terms of a tight-binding Heitler–London (atomic) scheme. Any changes from the gas-phase properties of the Rb atom are generally small and usually accounted for by second-order polarization and dispersion interactions with the host matrix (16).

(iii)   Obviously an intermediate situation (108) between (i) and (ii) may prevail. In this, the 5s wave function is still primarily confined to the neighborhood of the parent cation (Rb^+). However, increased overlap with the surrounding solvent requires that the electronic states of

the solute are best described in terms of a strongly perturbed atomic scheme (ii), or, alternatively, as a modified hydrogenic state (i). In the centrosymmetric representation of the paramagnetic state (Fig. 6), both these situations are accounted for in terms of the variation of the effective Bohr radius of the valence electron (16). The alternative scheme (53) recognizes a high electron density at the rubidium nucleus in terms of a "contact" ion-pair species (32), in which there is a significant degree of interaction between e_s^- and the outer 5s orbital of Rb^+, resulting in an appreciable atomic character.

(iv)   States (i) to (iii) *all* represent bound states, in which the excess electron is trapped in the reduced Coulombic field of the parent ion. If the polarization of the host solvent by the metal cation is sufficiently large, the valence electron will escape the Coulombic field and become ionized [Eq. (1)]. This spontaneous ionization† (which is, in fact, the dissolution process) is now comparable to the introduction of an excess electron into the pure solvent via an adiabatic process—for example, via photochemical or radiation processes (146). The properties of this electronic state are now determined by the factors responsible for the solvation of excess electrons in polar solvents, as outlined in Section II.

Having briefly discussed the various possibilities for matrix-bound paramagnetic states in these systems, we now review the main spectroscopic information regarding these distinguishable species.

2. Fluid Solutions

a. *Electron spin resonance studies.* Perhaps the most telling information regarding the nature of the paramagnetic species in these systems arises from ESR studies. The ESR spectrum of the isolated solvated electron consists of a single narrow line with a g_e factor close to the freespin value; e.g., in ammonia the resonance has a width of ~0.030 G and g_e = 2.0016 (98). Given the possibility of an interaction with an alkali cation (Fig. 6), an appreciable electron (spin) density can exist at the metal nucleus. Provided this electron–cation association complex has a sufficiently long lifetime, then a hyperfine interaction is possible (12, 26, 156), resulting in (2I + 1) lines in the ESR spectrum (I is the nuclear spin of the cation). In fact, the observation (2, 3, 168) of metal hyperfine splitting in metal–amine solutions provided the first unambiguous identification of the atomic stoichiometry [Eq. (4)] of one of the paramagnetic species in metal–amine solutions.

The striking effect of both the solvent and metal on the ESR spectra

† A related ionization process at high metal concentrations, involving the transition from localized to itinerant excess electrons, is discussed in Section IV.

of metal solutions (58) is illustrated in Fig. 7 for solutions of K, Rb, and Cs in three solvents. A simple ion-pairing treatment (21, 26) is quantitatively capable of predicting the form of the ESR spectrum in the wide variety of solvent systems. Briefly, two parameters are critical in determining the spectra obtained (26): the effective lifetime (τ_M) of the (primary) electron–cation encounter process,

$$M_s^+ + e_s^- \rightarrow (M_s^+, e_s^-)$$
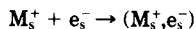
calculated from diffusion-controlled encounter theory, and A, the *metal* hyperfine coupling constant, expressed in hertz. The product $P_c = < \tau_M A >$ defines the form of the ESR spectrum. For the high-dielectric-constant solvents (NH_3, HMPA, etc.), $P_c \ll 1$ and a "time-averaged" signal of both paramagnetic species (e_s^-; M_s^+, e_s^-) is observed. In the lower-dielectric-constant solvents, $P_c \gg 1$, and the encounter lifetime is sufficiently long to permit the conversion of the "loose" ion pair (which must surely be the species formed in the *initial* encounter process) to a centrosymmetric species representing something like an "expanded" or solvated metal atom (Fig. 6). The latter species has the capability (in a low-dielectric-constant solvent) of a large hyperfine coupling to the metal nucleus. In Fig. 8 we show the established (26) P_c values for dilute solutions of metals in a variety of solvents.

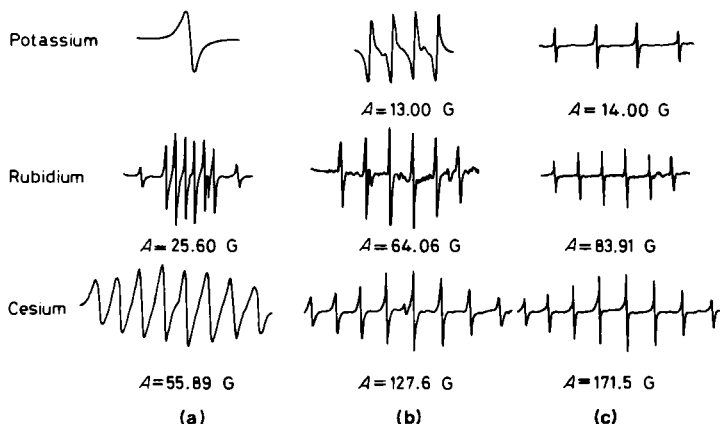The success of this type of approach is important since it emphasizes

FIG. 7. Electron spin resonance spectra of potassium, rubidium, and cesium in (a) methylamine, (b) ethylamine, and (c) propylamine; adapted from Dye and Dalton (58), with permission. Note the change in scale from pattern to pattern, as indicated by the (metal) hyperfine splittings given. Reprinted with permission from J. L. Dye and L. R. Dalton, *Journal of Physical Chemistry*, 71, 184 (1967). Copyright 1967 American Chemical Society.
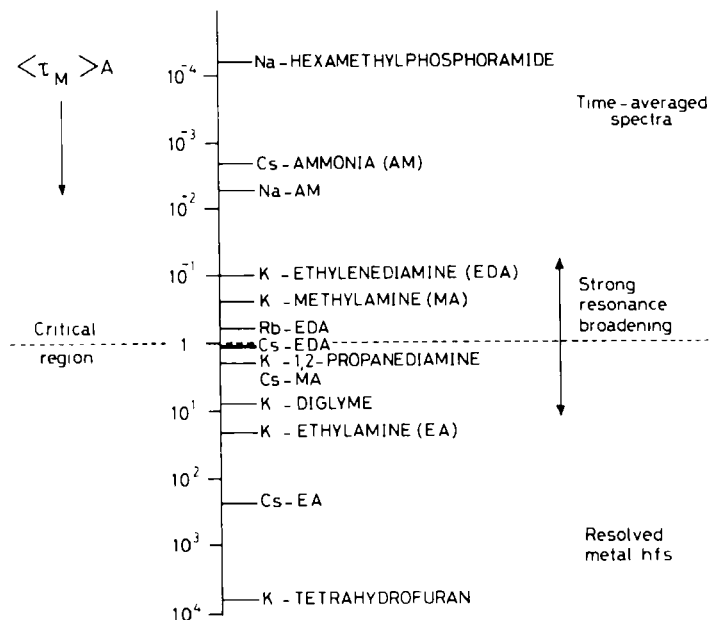
FIG. 8. Classification of ESR spectra (~296 K) of solutions of alkali metals in a variety of nonaqueous solvents: τ_M is the electron–cation encounter lifetime, and A is the metal hyperfine coupling constant, in hertz; THF = tetrahydrofuran, EA = ethylamine, DG = diglyme, MA = methylamine (~220 K), 1,2PDA = 1,2-propanediamine, EDA = ethylenediamine, AM = ammonia (~240 K).

once again that, despite the unique nature of e_s^- and the various types of association complexes formed with solvated metal cations, a standard ion-pairing treatment does indeed give a reasonable semiquantitative description of the magnetic and electrical properties of dilute solutions (26, 37, 164).

The separation (A) of the hyperfine lines in the ESR spectra of metal–amine, and metal–ether solutions represents a direct measure of the average s-electron (spin) density of the unpaired electron at the particular metal nucleus (12, 156). When this splitting is compared to that of the free (gas-phase) atom, we obtain a measure of the "percent atomic character" of the paramagnetic species. The percent atomic character in all these *fluid* systems increases markedly with temperature, and under certain circumstances the paramagnetic species almost takes on "atomic" characteristics (43, 53, 160). Figure 9 shows the experimental data for fluid solutions of K, Rb, and Cs in various amines and ethers, and also for frozen solutions (solid data points) of these metals in HMPA (17). The fluid solution spectra have coupling con-
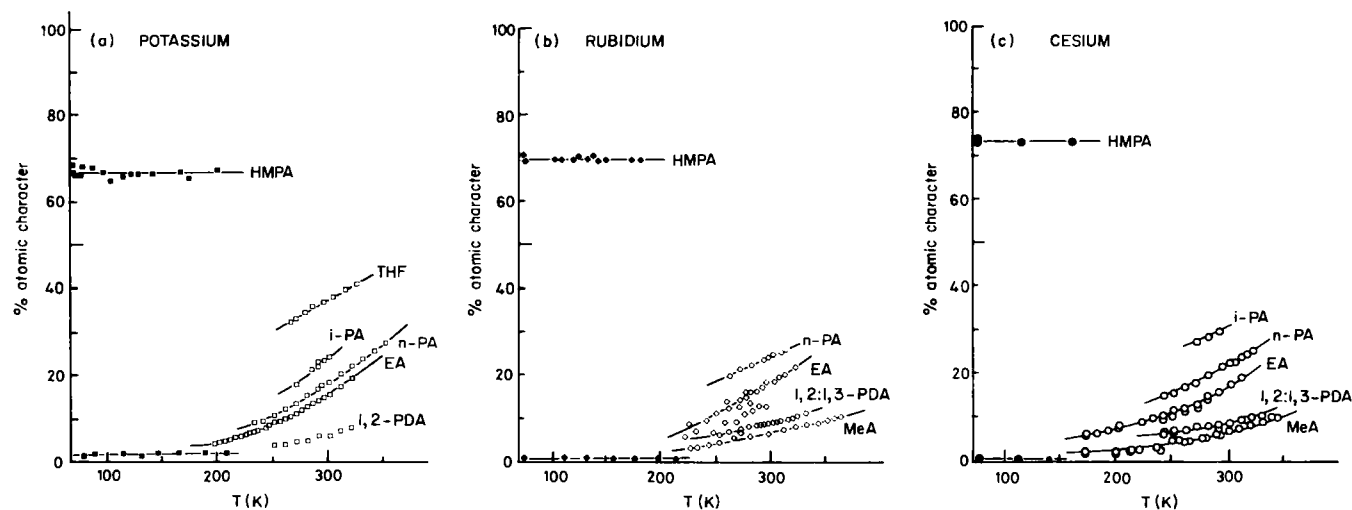
FIG. 9. Temperature dependence of the (metal) hyperfine coupling constant, expressed as percent atomic character, as a function of temperature for solutions of (a) potassium (^{39}K), (b) rubidium (^{85,87}Rb), and (c) cesium (^{133}Cs) in amines, ethers, and HMPA. The experimental data are from a variety of sources, and outlined elsewhere (16). Open symbols denote parameters from fluid solution studies; shaded symbols are from frozen solutions in HMPA. Solvent identification: as in Figure 8, and BuA = butylamine, i-PA and n-PA are isopropylamine and n-propylamine.

stants that are intermediate between values for the high and low
atomic character states identified in the frozen HMPA solutions, but
tend toward these values both in the high and low temperature ex-
tremes, respectively (this correlation between fluid and frozen solution
data is discussed in detail in Section III,B,4).

Figure 10b shows the extrapolation of the magnetic data (percent
atomic character) for Cs in various solvents (16, 17) to high tempera-
tures, while Figure 10a shows the corresponding g_e factors for Cs–
ethylamine solutions (128). Once again, the corresponding data ob-
tained from studies of frozen solutions of the respective metals in
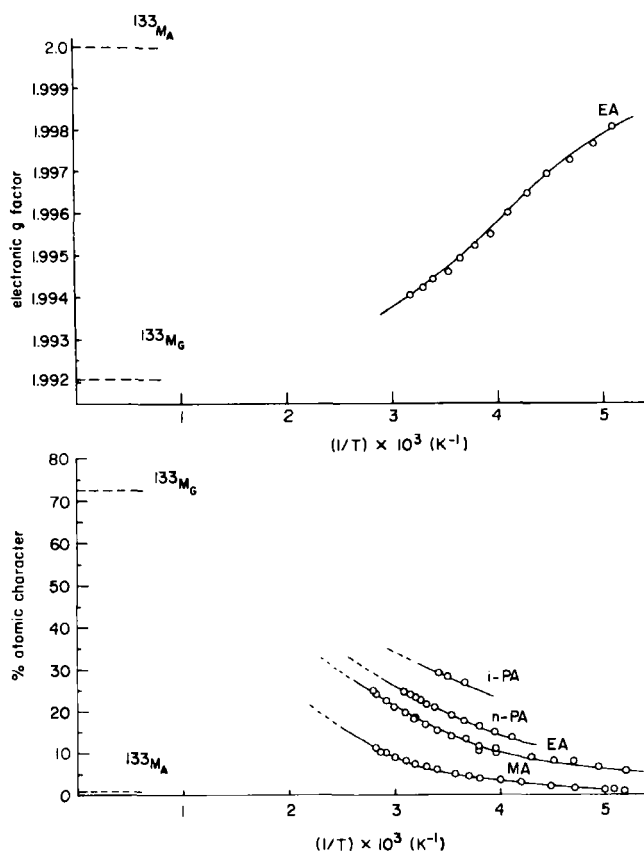HMPA are also included as limiting values at the high and low tem-

FIG. 10. Magnetic parameters for solutions of cesium-133 in various amines and
ethers, and in HMPA. Open symbols are for fluid solution studies (130). Dotted lines on
the ordinate show the limiting high- and low-atomic-character states observed in frozen
Cs–HMPA solutions (16). Solvent identification as in Fig. 8.

perature extremes. These types of considerations led to the postulate (30, 161) that the limiting (high-temperature) high atomic character state in the *fluid* metal–amine and metal–ether solutions is a *solvated* (Figs. 9, 10) rather than a "free" (i.e., 100% atomic character), alkali metal atom.

b. *Optical studies.* Optical spectra of fluid metal–amine and metal–ether solutions contain a band in the near infrared, at first sight somewhat similar in shape and position to the isolated e_s^- band in these solvents, and two additional bands at higher energies whose positions are dependent primarily upon the alkali metal (75, 150). One of these metal-dependent optical bands has been assigned (119) to solvated alkali metal anions (Section III,B,5), while kinetic studies (75) have demonstrated that the other, *transient* band (observed via first-detection techniques, e.g., pulse radiolysis) arises from the paramagnetic species of atomic stoichiometry, (M_s^+, e_s^-). The position of the (M_s^+, e_s^-) optical absorption exhibits (28, 148, 151, 153) a distinct *blue* shift from that of e_s^- observed in the same solvent (compare Section III,A,1 and Fig. 4 for dilute ammonia solutions). Furthermore, a close correlation has been established (28, 151) between the magnitude of this shift and the percent atomic character of the paramagnetic species (M_s^+, e_s^-), as determined by ESR studies. Figure 11 shows the available optical and ESR data for K and Cs states in a variety of host matrices (65). This
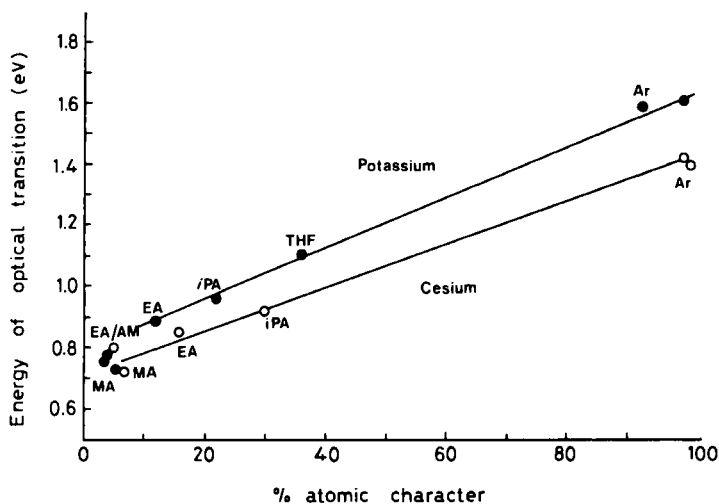

FIG. 11. Correlation of optical and ESR data for monomeric forms of potassium and cesium in a variety of host matrices. [From Edwards and Catterall (65); used with permission of Taylor and Francis, Ltd., *Philosophical Magazine.*]
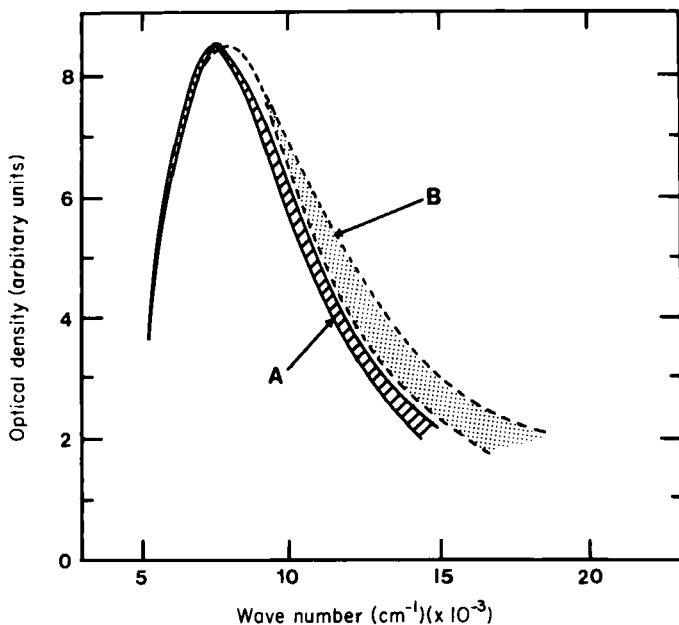
FIG. 12. Infrared optical absorption bands observed in ethylenediamine solutions: (A) spread in band shape of e_s^- observed by pulse radiolysis, (B) spread in band shape observed in alkali metal solutions. [Adapted with permission from W. A. Seddon and J. W. Fletcher, *Journal of Physical Chemistry*, **84**, 1104 (1980). Copyright 1980 American Chemical Society.]

correlation extends over the entire range from ion-pair-like species in the high-dielectric-constant solvents (e.g., NH_3) through the mono-meric, solvated atom states to the atomic variants found in the non-polar rare-gas matrices.

The role of ion pairing in producing a blue shift in the optical spec-trum may also extend to systems previously supposed to be metal-independent in dilute solutions. In an excellent and timely review, Seddon and Fletcher (*150*) have highlighted the recent advances made in the study of optical properties of dilute metal solvent systems, and at the same time reexamined the precise resolution and interpretation of metal-solution spectra. Figure 12 shows the optical spectra (*150*) at-tributed to e_s^- in ethylenediamine (EDA). The low-energy profile (A) encompasses the spread in band shape observed in pulse radiolysis studies of pure EDA. The high-energy profile (B) represents the range of published spectra observed in alkali metal solutions in EDA. Two ef-fects are noticeable: (i) a slight shift toward the blue in the band max-ima in the *presence* of alkali metal cations, and at the same time, (ii) a

significant broadening of the band, especially in the more concentrated alkali-metal solutions. Observation (i) is consistent with the general trend of a blue shift in the band maximum of e_s^- upon ion pairing (Fig. 11), while (ii) may, in part, be the result of ion-pair formation; there also remains the distinct possibility of an underlying contribution from (M_s^-). Clearly, a more quantitative assessment of the optical spectra of dilute metal–solvent systems must now follow from the approach taken by Seddon and Fletcher (*150*). In conclusion, we note also that the absorption spectra of (M_s^+, e_s^-) and (M_s^-) exhibit a certain asymmetry, similar to that observed for the isolated solvated electron.

3. Current Models for Paramagnetic States in Amine and Ether Solutions

Two conceptually different models have been proposed to explain the temperature dependence of the (metal) hyperfine coupling constant and electronic g_e factor in metal–amine and metal–ether solutions.

a. Multistate model. The multistate or dynamic model was originally developed by Hirota *et al.* (*95*) to explain the anomalous line-width variation of cation hyperfine lines in ion pairs of the type $M^+ R \cdot ^-$, where $R \cdot$ is an organic radical. The model was applied to metal solutions by Dye and co-workers (*43*) and by Catterall, Symons, and Tipping (*30*), and proposes that two or more paramagnetic species, each having different g_e factors and (metal)·hyperfine coupling constants, are in rapid equilibrium with each other. The individual species are assumed to have a structure that, to first order, is insensitive to temperature variations. The observed hyperfine coupling constant A is then represented by

$$A = \sum_i x_i A_i \tag{9}$$

where x_i and A_i are the mole fraction and hyperfine coupling constant for the ith state, respectively. In fluid solutions, individual states cannot be observed by ESR, and observed properties (A, g_e) represent a weighted average of those of the individual states. The temperature dependence of A then reflects the *changing relative populations of states*. The variations in line widths across the ESR spectra (Fig. 7) are interpreted in terms of the time-dependent modulation of the hyperfine interaction between the unpaired electron and the metal nucleus of the two (or more) magnetically inequivalent states of stoichiometry M.

b. Continuum model. In the continuum model of Bar-Eli and Tuttle (*2, 3*), a *single* centrosymmetric species is invoked to explain the metal

hyperfine coupling. The temperature variation in A then arises from the temperature-dependent changes in the solvation structure of the central metal ion. Inherent in the continuum model is a time-dependent modulation of the hyperfine coupling arising from the inter-conversion of nonequivalent states *within* the one state distribution (Fig. 13), which explains the anomalous line-width variation in the ESR. The model was put on a quantitative basis by O'Reilly and Tsang (*135*).

Figure 13 is a schematic representation of the anticipated distribution functions (number of states with a given hyperfine coupling constant) at high and low temperatures for the two models (*17*).

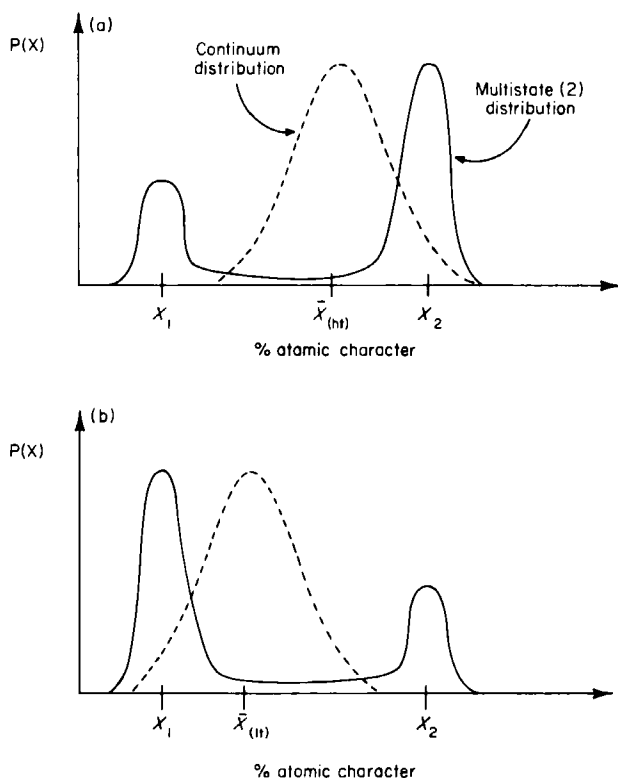The observation (*153*) of a *single* transient optical-absorption band

FIG. 13. A schematic representation of the multistate and continuum models for metal–amine and metal–ether solutions at (a) high and (b) low temperatures. The multistate picture shown here assumes, for simplicity, two species of atomic character X_1 and X_2. The continuum model suggests a single species with an atomic character of $\overline{X}_{(ht)}$ and $\overline{X}_{(lt)}$ at the extremes of high and low temperatures, respectively. P(X) is a measure of the number of states with a given percent atomic character.

from the cation–electron aggregate (M_s^+, e_s^-) in several amines and tetrahydrofuran, and its correlation (151) with ESR results (Fig. 11), would, at first, appear to contradict the multistate picture. However, in the series THF, dimethoxyethane, and the polyglycoldimethyl ethers (glymes), evidence was obtained (150) for the existence of *two* distinct optical bands resulting from the reaction of e_s^- with Na_s^+ to give two or more distinct cation–electron aggregates in equilibrium. This latter result is in accord with ESR multistate models.

The essential difference between the multistate and the continuum model rests upon the temperature dependence of the density of states (Fig. 13). An experimental distinction between the models may also be possible (21) from a study of genuine vitreous (quick-frozen) solutions, i.e., systems that, at low temperature, retain the appropriate fluid solution species existing *at* the freezing point. For these systems, the continuum model predicts a *single* species at low temperature with a low A value, while the multistate picture requires the superposition of spectra from two (or more) species: one (or more) in high abundance with a low A value, and at least one in lower abundance with a high value of A (Fig. 13).

For a variety of reasons (16, 21), we turned our attention to HMPA in the hope of obtaining *genuine* frozen solutions suitable for spectroscopic examination. Indeed, ESR studies of these rapidly frozen solutions revealed a rich variety of signals (16–23, 64, 65).

4. *Quenched* Metal–HMPA *Solutions*

A detailed discussion of the analysis and characterization of these signals is given elsewhere (17); here we quote typical results for illustrative purposes. A representative spectrum (21) at high machine amplification of a frozen rubidium–HMPA solution is illustrated in Fig. 14. Identified ^{85}Rb and ^{87}Rb resonances are indicated in the figure and the initial assignment summarized schematically. We have proposed (18, 19) a system of nomenclature that classifies states in terms of their percentage occupation of the outer metal (ns) orbital, labeling alphabetically from the lowest atomic character state (^xM_A, ~1%) to the highest (^xM_I, ~80%). Superscripts denote the mass number of the isotope.

From this type of analysis, it is possible to arrive at a distribution function (21) for the paramagnetic states in these vitreous solids, and a typical plot for ^{85}Rb species at liquid-nitrogen temperatures is shown in Fig. 15. This analysis has also recently been extended (17) to potassium and cesium solutions. The results clearly show the presence of
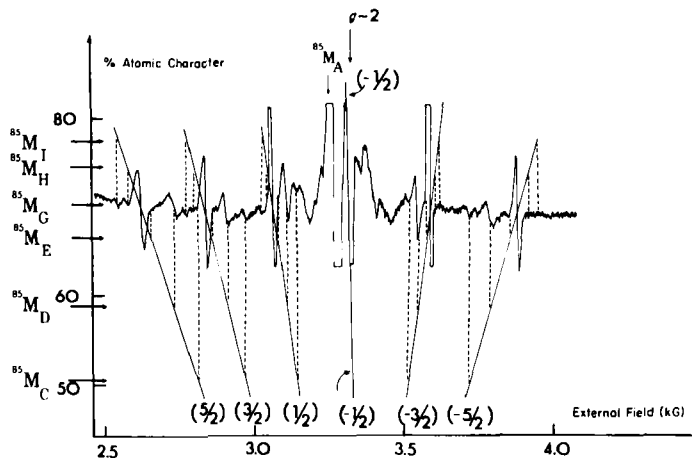
FIG. 14. Electron spin resonance spectrum of a frozen solution of rubidium in HMPA, at high machine amplification. The full lines show the variation of resonant field position with A for g_e = 1.99800, and a microwave frequency of 9.1735 GHz. The lines are anchored at the crossovers of the $^{85}M_G$ species (A = 251.3 G). Positions of the M_C, M_D, M_E, M_G, M_H, and M_I absorptions are indicated. Reprinted with permission from R. Catterall and P. P. Edwards, *Journal of Physical Chemistry*, **79**, 3010 (1975). Copyright 1975 American Chemical Society.

FIG. 15. The experimental distribution function for paramagnetic states identified in frozen rubidium–HMPA solutions at liquid-nitrogen temperatures (*21*). Reprinted with permission from R. Catterall and P. P. Edwards, *Journal of Physical Chemistry*, **79**, 3010 (1975). Copyright 1975 American Chemical Society.
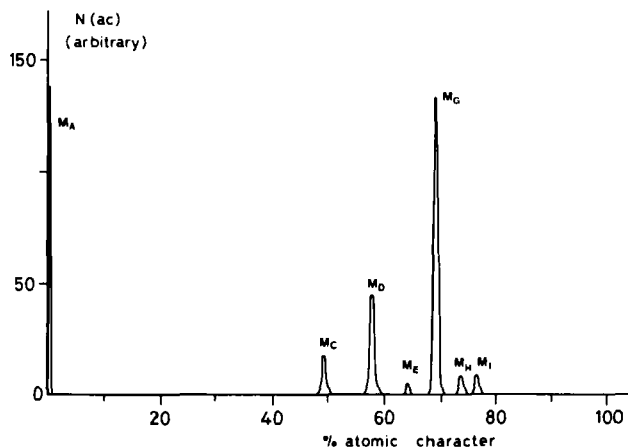
centers differing widely in percent metal (ns) character. In addition, the coupling constants observed in fluid metal–amine and metal–ether solutions are always intermediate between values for the ^xM_G and ^xM_A species in frozen metal–HMPA solutions, but tend toward these values, respectively, in both the high and low temperature extremes. These results obviously confirm the presence of a distribution of paramagnetic states in these quick-frozen solutions. Unfortunately, the underlying problem here is whether these species observed in the vitreous solid are indeed representative of a variety of paramagnetic states in the liquid solution as well (53). This is a difficult question to answer. However, two major features (17) of these studies are important in this regard. The first is the remarkable reproducibility of the results for the frozen solutions (17). The second aspect concerns the strong correlation in the ESR parameters (A and g_e) for both fluid metal–amine and metal-ether solutions, and frozen metal–HMPA solutions. This is highlighted in Fig. 16, where we plot the variation of the electronic g_e factor shift [$\Delta g_e = g_e$ (free atom) $- g_e$] as a function of percent atomic character for the species M_A to M_H identified in frozen HMPA solutions, together with the corresponding data for fluid amine and ether solutions. For all metals studied, the electronic g_e factor moves smoothly away from the free atom value as A moves toward the atomic value. This behavior is indeed strong evidence that the limiting high-temperature paramagnetic state in the fluid solutions is the *solvated* metal atom. In addition, the maximum observed g_e shifts for each metal correlate well (21) with the (metal) spin–orbit coupling constants λ_{so}. Similarly, measured electron spin–lattice relaxation times (24, 25) for the solvated alkali metal atoms in frozen metal–HMPA solutions show a strong correlation with the magnitude of the spin–orbit coupling constant (Table I).

In these vitreous solids, then, the *entire* spectrum of possible

TABLE I

SPIN–LATTICE RELAXATION DATA FOR ALKALI METAL ATOMS[a]

Metal	λ_{so} (eV)[b]	T_{1e} (sec)	T_{2e} (sec)
Na	1.41×10^{-3}	$>5 \times 10^{-2}$	$\sim1 \times 10^{-8}$
K	4.75×10^{-3}	6.4×10^{-2}	1.3×10^{-8}
Rb	1.95×10^{-2}	1.5×10^{-3}	1.2×10^{-8}
Cs	4.55×10^{-2}	2.0×10^{-4}	1.3×10^{-8}

[a] From Catterall and Edwards (24, 25).

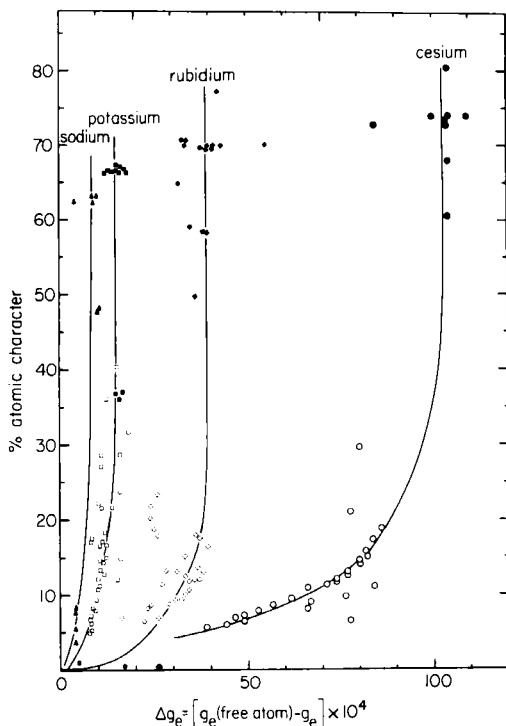[b] 1 eV $\cong 1.6021 \times 10^{-9}$ J.

Fig. 16. Correlation of percent atomic character with Δg_v for frozen solutions of sodium, potassium, rubidium, and cesium in HMPA, and for fluid solutions in various amines and ethers. Reprinted with permission from R. Catterall and P. P. Edwards, *Journal of Physical Chemistry,* **79,** 3010 (1975). Copyright 1975 American Chemical Society. Frozen M–HMPA solutions are shaded symbols. Open symbols are fluid amine and ether solutions.

electron–cation aggregates (Section III,B,1) appear to exist. The high-atomic-character states ($^{85}M_C$ to $^{85}M_I$, Fig. 15) are best viewed as solvated metal atoms (Fig. 6).

The low-atomic-character state ($^{85}M_A$) can be interpreted (*19*) in terms of the loose ion-pair picture (Fig. 6), or alternatively, as a large-radius monomeric state [a_H^* estimated (*17*) to be in the region 10–15 Å]. Experimental magnetic parameters and unpaired electron spin densities at the metal nucleus for the ^XM_A species are shown in Table II.

Observed line widths are metal dependent. However, values of $|\psi_{(0)}|_M^2$, the unpaired electron (spin) density at the metal nucleus, *are approximately independent of the metal atom for potassium, rubidium, and cesium species.* As such, the states $^XM_A(X = 39, 85, 133)$ are best described as *true* hydrogenic states in this disordered medium.

TABLE II

EXPERIMENTAL MAGNETIC PARAMETERS FOR THE ^XM_A (X = 39, 85, 133) STATE IN
LOW-TEMPERATURE ALKALI METAL–HMPA GLASSES[a]

Isotope	I	g_e	ΔH (G)	A (G)	$10^{24}\|\psi_{(0)}\|^2_M$ (electrons cm^{-3})[b]
^{39}K	$\frac{3}{2}$	2.0018	4.9 ± 0.3	0.80 ± 0.1	0.073 ± 0.007
^{85}Rb	$\frac{5}{2}$	2.0009	9.4 ± 0.5	1.48 ± 0.1	0.065 ± 0.005
^{133}Cs	$\frac{7}{2}$	1.9994	14.9 ± 0.8	1.85 ± 0.05	0.060 ± 0.006

[a] From Catterall and Edwards (18, 19).

[b] For comparison purposes, $|\psi_{(0)}|^2$ atomic for the alkali atoms in question is: ^{39}K, 7.4790 × 10^{24}; Rb, 15.8225 × 10^{24}; ^{133}Cs, 26.4508 × 10^{24} (electrons cm^{-3}).

As outlined in Section III,B,1, these states forfeit any parentage in the electronic states of the gas-phase (parent) alkali atoms.

5. Diamagnetic States: Ion Triples to Alkali Metal Anions

Perhaps the most striking characteristic of metal–amine and metal–ether solutions that sets them apart from metal–ammonia solutions is the metal-dependent optical-absorption band that occurs at higher energies than the infrared band associated with e_s^- (51, 75, 150). This shifts progressively to higher energies for solutions of Cs, Rb, K, and Na in a given solvent (Fig. 17). The metal, temperature, and solvent dependence of this band prompted Matalon, Golden, and Ottolenghi (119) to suggest that the species responsible in amine solutions
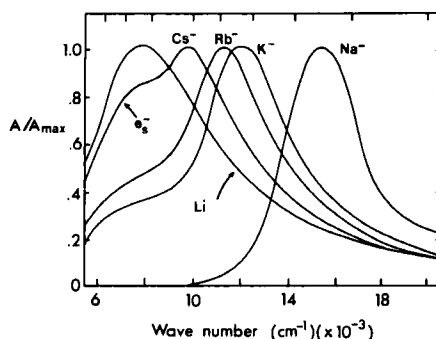

FIG. 17. Optical spectra of lithium, sodium, potassium, rubidium, and cesium in ethylenediamine with identification of absorption peaks of Na$^-$, K$^-$, Rb$^-$, Cs$^-$ and e_s^-. Absorption for e_s^- is taken from pulse radiolysis studies. [Taken from Fig. 1 of Dye (51); used with permission of Verlag-Chemie, *Angew. Chem. Int. Ed. Engl.*]

were alkali metal anions, and that the transitions were similar to the charge-transfer-to-solvent (CTTS) bands of I⁻ The term alkali metal anion refers to a spherically symmetric species with two electrons in the outer s-like orbital centered on the metal. However, this is only one of several possibilities open to a diamagnetic cluster of two electrons and a cation, and Fig. 18 is a schematic representation of the various species. Indeed in a "good" solvent such as ammonia, we expect (53, 143) this spin-paired species to resemble a loose triple ion, since a wide variety of properties are essentially unaffected by the electron–electron interaction (Section III,A,2). However, in the low-dielectric-constant solvents the evidence for a spherically symmetric alkali metal anion species has accummulated steadily over the last decade (51). In addition, the existence of alkali metal anions in the gas phase has been recognized for some time (50). In 1974, Dye and co-workers (56, 162) isolated and characterized a crystalline salt of the sodium anion. When a saturated solution of sodium metal in ethylamine in the presence of a cation-complexing agent (for example, bicyclic diamino ether, or "crypt") is cooled, gold-colored crystals form, whose structure corresponds to a sodium cation trapped in the crypt and a sodium anion outside (Fig. 19). More recent studies have also revealed the existence of alkali metal anions in thin solid films formed by evaporation of metal–ammonia solutions containing cation-complexing agents (42).

The NMR spectra of Na⁻, Rb⁻, and Cs⁻ have now been reported (52, 56). The chemical shift of Na⁻, large and diamagnetic, is the same as that calculated for the gaseous anion and is essentially independent of solvent. The apparent absence of a large paramagnetic shift of Na⁻ upon solvation, and the solvent independence of the peak position, have been cited (56) in support of a model in which the solvent is excluded from the region occupied by the sodium 2p electrons. However, recent studies (20) of the photodetatchment of electrons from K⁻ and Rb⁻ in HMPA glasses at low temperature reveal a significant degree of solvation in the alkali anion species. The overall conclusion (20, 52) must be that the alkali metal anion in these systems is a distinct, centrosymmetric species, with the two valence electrons residing in an expanded ns orbital on the metal.

The existence of metal anions in these nonaqueous systems is not confined to elements of group IA of the Periodic Table. Peer and Lagowski (137) have recently presented spectroscopic evidence for the existence of the auride ion Au⁻ in liquid ammonia, while Dye (51) has recently given an extensive assessment of the stability of crystalline salts of a variety of possible metal anions.

2M (ATOM)

2M⁺ₛ   +   e⁻ₛ

TRIPLE ION SPECIES

METAL ANION SPECIES

e⁻   M⁺   e⁻   e⁻ M⁺ e⁻   M⁻   OR   M⁻   M⁺

LOOSE TRIPLE ION   CONTACT TRIPLE ION   SOLVATED ALKALI
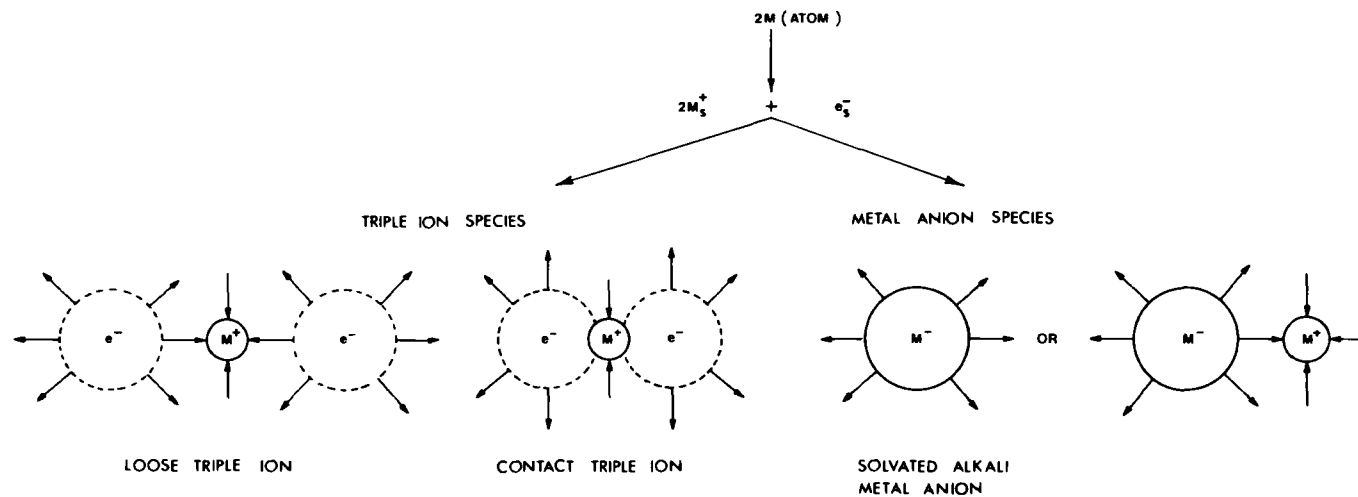   METAL ANION

FIG. 18. Diamagnetic electron–cation clusters in metal solutions. [Adapted, in part, from Dye (53); used with permission of Pergamon Press.]
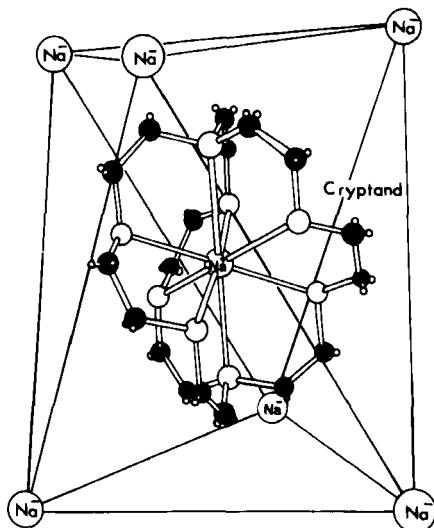
FIG. 19. Structure of the central Na^+,2,2,2-cryptand ion and the placement of the surrounding six Na^- ions in the Na^+,2,2,2-cryptand $\cdot$ Na^- crystal. (From Anions of the alkali metals, J. L. Dye. Copyright © 1977 by Scientific American, Inc. All rights reserved.)

IV. Concentrated Solutions and the Nonmetal-to-Metal Transition

In the preceeding sections, we have seen that the dielectric constant plays an important role in the binding energy of a localized-electron state—either isolated solvated electrons (Section II) or electron–cation aggregates (Section III). It is therefore particularly instructive to study its variation as the metal concentration is increased. Such measurements were carried out on sodium–ammonia solutions at 1.2, 5.4, and 10 GHz by Mahaffey and Jerde (117), and by Breitschwerdt and Radscheit (8). Over the concentration range 0.1 to 1 MPM, the results at 10 GHz (shown in Fig. 20) exhibit a very rapid increase to a value of nearly 100 before falling off to large negative values characteristic of Drude behavior for metals. Such a "dielectric catastrophe" was indeed the basis of the first consideration (34) of the nonmetal-to-metal (NM-M) transition in sodium–ammonia solutions by Herzfeld (93) in 1927. Stated simply, the dielectric constant goes to infinity at the metallic onset; the resultant binding energy on the (isolated) electron vanishes, and the system acquires metallic status! Over the composition range 0.1 to 10 MPM in sodium–ammonia solutions, the electrical conductivity increases by approximately four orders of magnitude (73, 94), and in the vicinity of the saturation point, it reaches a value exceeding that of liquid mercury (equivalent conductivity, $-33°C$,
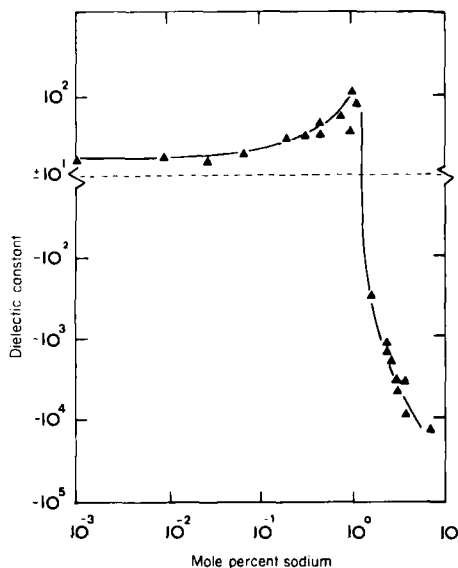
FIG. 20. The real part of the microwave frequency (10 GHz) dielectric constant as a function of sodium metal concentration at 298 K in sodium–ammonia solutions. *Note the break in the ordinate.* [Adapted from Mahaffey and Jerde (*117*); used with permission from the American Physical Society, *Reviews of Modern Physics.*]

Na–NH$_3$, 1.02×10^6 ohm^{-1} cm^2 mol^{-1}; for Hg, 0°C, 0.16×10^6 ohm^{-1} cm^2 mol^{-1}). In the intermediate composition range 1 to 7 MPM, a NM-M transition occurs, and changes in the electronic, thermodynamic, and mechanical properties of the system are equally impressive (*35, 37, 124, 154*). A detailed discussion of the concentration dependence of various properties of metal–ammonia solutions is given in the book by Thompson (*164*). In addition, a recent review (*60*) at Colloque Weyl V also summarizes the available data for lithium–methylamine solutions (*10, 11, 63, 127, 128, 166*).

Our canvas here is to provide a qualitative description of current models for the NM-M transition, developed for both metal–ammonia and metal–methylamine solutions. For this purpose we also draw upon interpretations from other systems in which the transition from localized to itinerant electron regimes is well recognized (*78*).

A. MODELS FOR THE NONMETAL-TO-METAL TRANSITION

1. The Herzfeld Theory of Metallization

In 1927, K. F. Herzfeld published a paper (*93*) in which he proposed a simple criterion for determining when an element or system will ex-

hibit true metallic characteristics. On classical grounds, Herzfeld argued that the characteristic frequency of bound electrons, representing a measure of the force holding the electron in the free atom, is diminished at high electron densities to the value

$$\nu = \nu_0(1 - R/V)^{1/2} \tag{10}$$

where ν_0 is the characteristic frequency in the isolated (low electron concentration) species, R is the molar refractivity, and V is the molar volume.

If $(R/V) = 1$, the resultant force on the localized electron vanishes, the electron is set free, and the system acquires metallic status. The previous statements may be recast in slightly different form using the venerable Clausius–Mossotti relationship (81), where

$$R/V = (n^2 - 1)/(n^2 + 2) \tag{11}$$

and n is the index of refraction, and n^2 is the optical dielectric constant.

When the condition $(R/V) = 1$ is fulfilled, the refractive index/dielectric constant goes to infinity, and we have a NM-M transition. The Herzfeld criterion when applied to metal–ammonia solutions does indeed predict (67, 93) that localized, solvated electrons are set free by mutual action of neighboring electrons at metal concentrations above ~4–5 MPM, and measurements (Fig. 20) similarly indicate a dielectric catastrophe in this concentration range. The simple Herzfeld picture has recently been applied by Edwards and Sienko (70) to explain the occurrence of metallic character in the Periodic Table.

2. The Mott Transition

Mott's major work (124–126) on the transition to the metallic state in simple metals has for a long time been used as a framework for the description of the NM-M transition in metal–ammonia solutions (37, 164, 165).

Consider a monovalent metal such as sodium (125). Each sodium atom carries with it one valence (3s) electron. The lower half of this band is then half filled. As far as a conventional picture is concerned (139), the 3s band is half filled and the valence electrons are therefore itinerant and move freely about the system. If we now increase the internuclear distance, there is a reduction in the width of the 3s band. Ultimately, as common sense would have it (125, 126), the band reduces to the discrete s level of the *isolated* sodium atom. Metallic con-

duction is no longer possible, although according to the band-model approximation we still have a half-filled band and therefore metallic conduction should still be maintained! The band-model approximation thus breaks down for "narrow" bands in which there is considerable electron–electron correlation (86, 87, 124). In a number of papers beginning in 1949 (124–126), Sir Nevill Mott addressed this fundamental problem. In Mott's view, the transition from metallic to nonmetallic regimes is sharp—indeed, first order: electrons are *either* localized in distinct regions of space, *or* itinerant. Figure 21 contrasts (165) the standard (band picture) view of the conductivity variation with those to Mott's.

Mott first gave an estimate (125) of this critical density at the NM-M transition in terms of the screening properties of an itinerant electron gas. The "Mott criterion" is

$$n_c^{1/3} a_H^* \geqslant 0.25 \qquad (12)$$

where n_c is the critical concentration of centers, and a_H^* is an effective radius for the isolated (localized electron) state. From an extensive analysis of experimental data for disordered materials, Edwards and Sienko (68) have recently found that a particular (scaled) form of the Mott criterion exhibits an apparent universality, in that the relation

$$n_c^{1/3} a_H^* = 0.26 \pm 0.05 \qquad (13)$$

predicts the critical concentration for the onset of metallic character for systems around the range of $\sim 10^9$ in critical densities (or alternatively
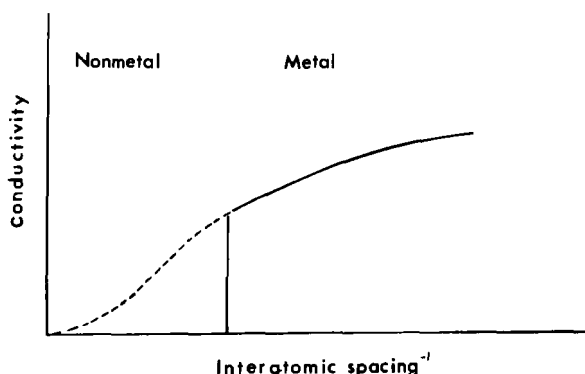

FIG. 21. A comparison of the anticipated changes in conductivity with atomic spacing from a conventional viewpoint (dashed line) and that of Mott. The abscissa is the reciprocal of the interatomic spacing. [Adapted from Thompson (165), with permission.]

600 Å in a_H^*) provided a_H^* is obtained directly from *experimental* parameters that characterize the localized electron state. The data (*64, 68, 69*) for metal solutions in ammonia, methylamine, and HMPA are included in Fig. 22. Inherent in the Mott picture (*124*) is a *major* change in the *thermodynamic properties* of the solutions in the transition region. This important feature is discussed in Section IV,B.
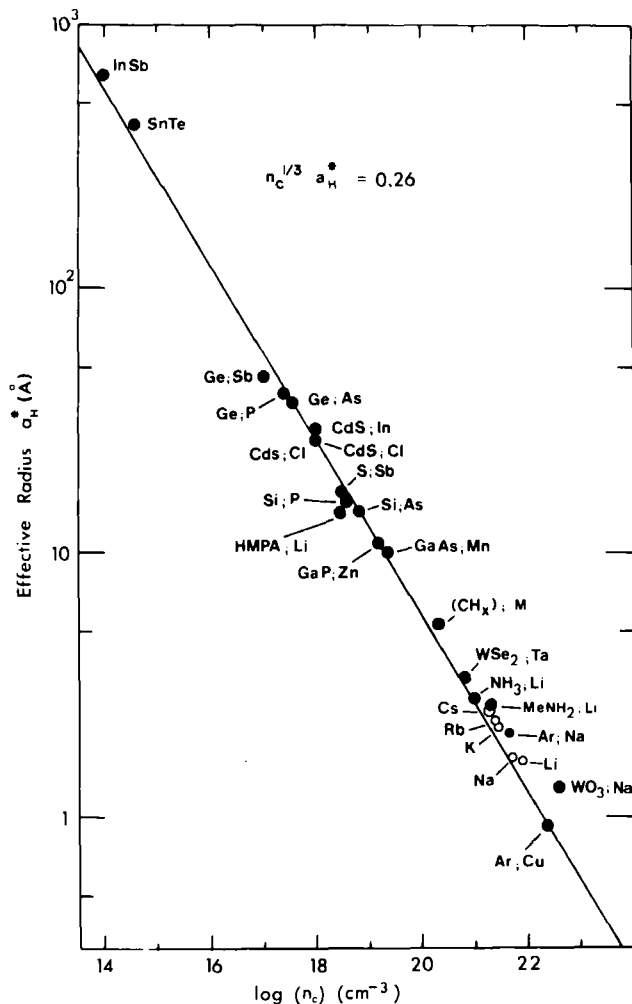

FIG. 22. The nonmetal-to-metal transition: a logarithmic plot of the effective radius a_H^* of the localized-electron state versus the critical (electron) concentration for metallization, n_c, in a variety of systems. [Adapted from Edwards and Sienko (*68*), and used with permission from the American Physical Society, *The Physical Review (Solid State)*.]

3. Inhomogeneous Picture for the Transition

The fundamental basis of Mott's picture for the NM-M transition in metal–ammonia solutions is that the system is essentially homogeneous (and slightly disordered) for temperatures sufficiently far removed from the consolute temperature for phase separation. An alternative model has been advanced by Cohen and Jortner (35, 36). Their description assumes that solutions in the transition range are microscopically inhomogeneous, consisting of highly concentrated regions with metallic conduction and dilute regions with electrolytic conduction. The dilute and metallic domains themselves are of constant and well-defined concentration, 2.3 and 9 MPM, respectively. An increase in the overall metal concentration ultimately leads to a finite fraction of the material being connected as a conduction path leading across the sample (35, 146) (Fig. 23). A percolation problem was then posed, and the approach utilized to account (almost quantitatively) for numerous transport properties (35, 36). In contrast to the Mott picture (123), the NM-M transition here is essentially continuous; the particular interpretation used by Jortner and Cohen (35, 36) puts the percolation threshold near 3.5 MPM. However, the overriding question (122, 123) is whether we have any direct experimental evidence for a microscopic structure in which the local concentration fluctuates between the two well-defined boundaries. Damay and Chieux have recently carried out small-angle neutron scattering (SANS) studies on sodium and lithium solutions in liquid deuteroammonia at concentrations near 4 MPM, from the liquid–liquid critical temperature up to room temperature (44). Their complete SANS data could apparently be attributed to concentration fluctuations on purely thermodynamic grounds for systems close to a critical point. However, the more recent heat capacity studies by Steinberg et al. (158) reopen the important question of the validity
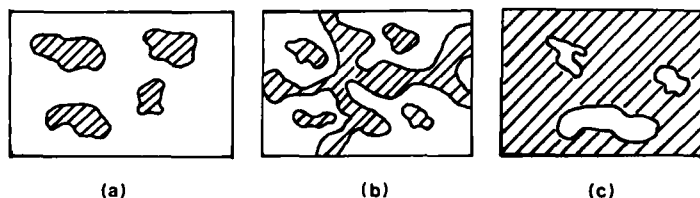

(a)   (b)   (c)

FIG. 23. Illustration of the nonmetal-to-metal transition according to the percolation picture of Cohen and Jortner (see text). Solvent regions of high metal concentration are shaded. Metallic regions grow with increase of metal concentration. (a) Below the percolation threshold there are isolated metallic regions and no conductance. (b) Above the percolation threshold a metallic path crosses the material and conduction occurs. (c) Above a certain critical concentration, the insulating regions are disjoint.

of a percolation hypothesis for the transition region in metal–ammonia solutions.

B. LIQUID–LIQUID PHASE SEPARATION AND THE NONMETAL-TO-METAL TRANSITION

If a solution containing approximately 4 mole percent sodium in ammonia is cooled below −42°C (231 K) a remarkable liquid–liquid phase separation occurs (*33, 155*). The solution physically separates into two distinct layers—a low-density, bronze metallic phase that floats out on top of a more dense, less concentrated dark-blue phase. The first experimental observation of this striking phenomenon in sodium–ammonia solutions was made by Kraus (*109, 110*) in 1907; more recent studies have mapped out the phase coexistence curves for a variety of alkali and alkaline earth metals in liquid ammonia, and these are delineated and discussed elsewhere (*164*).

In 1958, Pitzer (*141*), in a remarkable contribution that appears to have been the first theoretical consideration of this phenomenon, likened the liquid–liquid phase separation in metal–ammonia solutions to the vapor–liquid condensation that accompanies the cooling of a nonideal alkali metal vapor in the gas phase. Thus, in sodium–ammonia solutions below 231 K we would have a phase separation into an insulating vapor (corresponding to matrix-bound, localized excess electrons) and a metallic (matrix-bound) liquid metal. This suggestion of a "matrix-bound" analog of the critical liquid–vapor separation in pure metals preceeded almost all of the experimental investigations (*41, 77, 91, 92*) into dense, metallic vapors formed by an expansion of the metallic liquid up to supercritical conditions. It was also in advance of the possible fundamental connection between this type of critical phenomenon and the NM-M transition, as pointed out by Mott (*125*) and Krumhansl (*112*) in the early 1960s.

The precise nature of the electronic interactions between centers must obviously change dramatically at the NM-M transition, e.g., from van der Waals type interaction to metallic cohesion (*112*). These gross changes in electronic properties at the transition are sufficient to noticeably influence the thermodynamic features of the system (*86, 87*). The conditions therefore appear highly conducive for a *thermodynamic phase transition* to accompany the *electronic transition* at the critical density. In fact, the transition to the metallic state in metal–ammonia solutions is accompanied by a decrease in both enthalpy and entropy (*146, 149*), and it has been argued convincingly (*124, 125*) that the phase separation in supercritical alkali metals and metal solutions is

indeed a consequence of these changes in thermodynamic functions (Fig. 24).

In a recent communication (70), we have reexamined Pitzer's early hypothesis in the light of the considerable advances made recently both in the theoretical and experimental study of supercritical fluid alkali metals (41, 77), doped semiconductors (78), and metal–ammonia and metal–methylamine (60, 166) solutions. The latter systems are particularly instructive (70). Preliminary data (10) for the lithium–methylamine system suggests that phase separation occurs around 15–16 MPM, compared to approximately 4 MPM in lithium–ammonia solutions (Fig. 25). In both solvent systems, this critical composition also marks the onset of the NM-M transition for $T > T_c$ (critical consolate temperature). Table III is a collation of critical (consolate) densities in lithium–ammonia, sodium–ammonia, and lithium–methylamine solutions, together with the observed critical densities of the pure alkali metals and the corresponding estimates of the Mott criterion ($n_c^{1/3}$ a_H^*) for all systems under investigation (70). These condensation phenomena observed in both gaseous and matrix-bound systems appear to be closely related. Furthermore, they are significantly correlated in that, in all cases, critical (metal) densities at the metallic onset ($T > T_c$), or at the phase separation limit ($T < T_c$) are in good agreement with the Mott criterion [Eq. (13)]. Pitzer's suggestion (141),
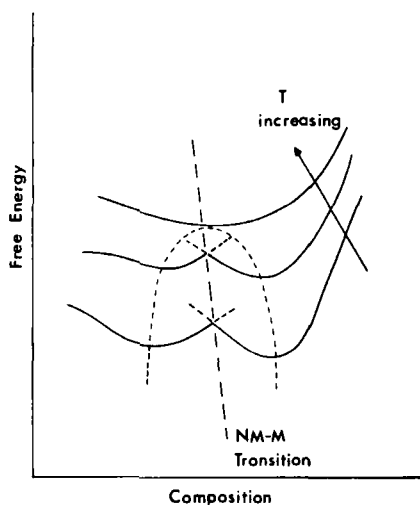

FIG. 24. The electronic and thermodynamic phase transitions at the nonmetal-to-metal transition: a schematic representation of the free energy of a metal–ammonia solution in the temperature range of the miscibility gap, showing the NM-M transition as a function of metal concentration for increasing temperatures.
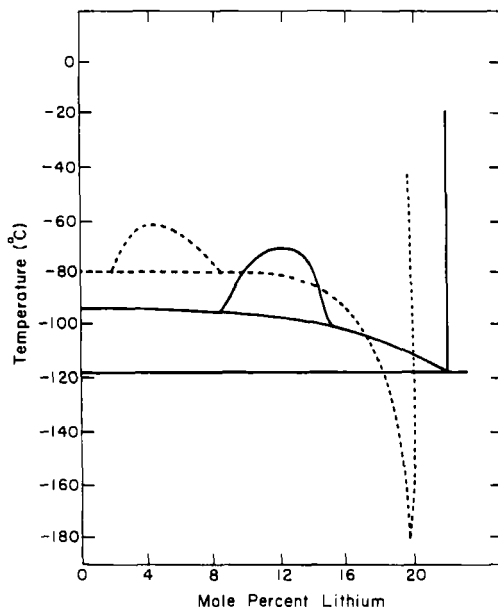
FIG. 25. A comparison of phase relations in the systems lithium–ammonia (– – –) and lithium–methylamine (———). The latter is the tentative phase diagram based on preliminary studies (10).

that phase separation in metal–ammonia solutions is the analog within the liquid ammonia medium of the liquid–vapor separation of the pure metal, does indeed represent a particularly apt description of the phenomenon (70).

C. Expanded-Metal Compounds

The lithium–ammonia phase diagram shows a deep pseudoeutectic (Fig. 25) at approximately 20 MPM and 88.8 K, which signals the appearance of a compound, tetraamminelithium(0) of stoichiometry $Li(NH_3)_4$. A great deal of evidence, both direct and indirect, has now been amassed that shows that a true compound, rather than a simple eutectic solid, does indeed exist at low temperatures (118, 164). Recent studies of metal–ammonia compounds suggest that they may crystallize in unusual structural arrangements (82, 83, 167). For example, the compound $Ca(ND_3)_6$ may possess a novel ND_3 geometry in which the ammonia molecules are nearly planar and have two inequivalent sets of deuterons, with one N–D distance being rather short (~0.9 Å), while the other two are extremely long (~1.4 Å) (82). Whatever the pecu-

TABLE III

THE MOTT CRITERION FOR METAL SOLUTIONS AND EXPANDED FLUID
METALS[a]

System	n_c (cm^{-3})	a_H^* (Å)	$n_c^{1/3}a_H^*$
I. Supercritical alkali metals[b]			
Li	9.43×10^{21}	1.59	0.34
Na	5.48×10^{21}	1.71	0.30
K	2.89×10^{21}	2.16	0.31
Rb	2.40×10^{21}	2.29	0.31
Cs	1.9×10^{21}	2.52	0.32
II. Metal solutions[c]			
Li–NH$_3$ (209 K)	9.94×10^{20}	2.83	0.28
Na–NH$_3$ (231 K)	9.03×10^{20}	2.88	0.28
Li–MeNH$_2$ (~200 K)	1.85×10^{21}	2.60	0.32

[a] Full details given in Ref. 69.

[b] Values of n_c at the gas–liquid critical point; a_H^* derived from radii corresponding to the principal maxima in the radial distribution functions $[r^2\psi^2(r)]$, using relativistic wave functions.

[c] Values of n_c taken at the concentration of the liquid–liquid phase separation; a_H^* derived from the adiabatic cavity model for the solvated electron (see Section II).

liarities of the local structure in the complexes, the most appealing overall description (154) of the solid compound is that of an "expanded metal." In this, the ammonia simply takes the role of a space-filling diluent, effectively increasing the Li–Li separation relative to that in the pure metal. This dilution effect highlights one of the great attractions (66) of these materials, namely, that via pertinent choice of solvent these low-electron-density materials could be tailored in such a fashion as to move them toward the metal–nonmetal transition.

Edwards, Lusis, and Sienko have recently reported an ESR study (60) of frozen lithium–methylamine solutions which suggests the existence of a compound tetramethylaminelithium(0), Li(CH$_3$NH$_2$)$_4$, bearing all the traits (60) of a highly expanded metal lying extremely close to the metal–nonmetal transition. Specifically, both the nuclear-spin and electron-spin relaxation characteristics of the compound, although nominally metallic, cannot be described in terms of the conventional theories of conduction ESR (6, 15, 71) and NMR in pure metals (60, 96, 169).

The use of cyclic (crown) polyethers and cryptates to enhance metal solubilities also opens up many interesting possibilities for studying expanded-metal compounds in the low-dielectric-constant solvents

(51). In addition, thin solid films obtained by evaporation of metal–ammonia solutions that contain a cation complexing agent (cryptand) have transmission spectra that suggest the existence of expanded metals in these systems (42).

V. Concluding Remarks

The fundamental theme for this review was the attempt to illustrate the "flavor" of current research in this area. If one were to summarize (62, 146) the present status of our knowledge of these remarkable systems, it might be that most of the properties of excess electrons in solution can be interpreted in terms of models that are (qualitatively) easily understood, but quantitatively evaluated only with considerable effort. This is, indeed, an observation pertinent not only to metal solutions, but to inorganic chemistry in general!

We conclude this review as we have started it—with a brief reference to unpublished work by Sir Humphry Davy:

During the course of many laborious experiments (1808–1809) on the action of dry gaseous ammonia with molten potassium (Fig. 1), Davy speculated briefly on the possible reaction at the metal interface, questioning "whether any substances can be formed which will not absorb Ammonia." Unfortunately, Davy's intense activity during this period led to considerable fatigue, and (136) "a most severe fit of illness, which for a time caused an awful pause in his researches, broke the thread of his pursuits, and turned his reflections into different channels."

Appendix

The purpose of this section, added in proof, is to include certain work published since the review was completed.

The first observation of the NMR spectrum of Na^- in a metal solution without added cation-complexing agents has recently been reported (65a). The rationale behind this observation was that the solvent HMPA by itself appeared to fulfill many of the requirements generally sought from macrocyclic complexing agents: high solubility via cation complexation, stability to electron reduction, weak anion solvation, etc. The NMR spectrum of Na^- in fluid Na–HMPA solutions, shown in Fig. 26, exhibits precisely the same chemical shift as that observed for Na^- in solutions of Na in anhydrous methylamine and ethylamine in the presence of 2,2,2-cryptand. The metal anion here is truly "gas-like" in
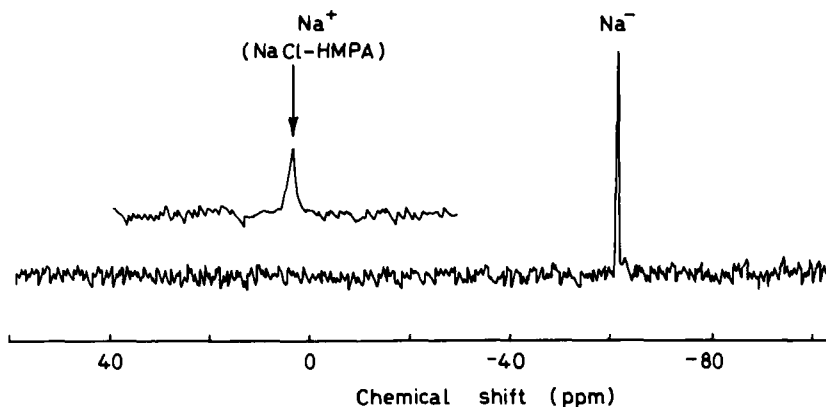
FIG. 26. The ^{23}Na NMR spectrum of Na$^-$ in a solution of sodium in HMPA (65a).

that the sodium 2p electrons are effectively shielded from solvent interactions by the presence of two spin-paired electrons in an almost unperturbed 3s orbital on the metal.

The magnetic susceptibility data for metal–ammonia solutions cited earlier (see Fig. 5) have now appeared in the chemical literature (88a). For metal–ammonia solutions at −65°C, the spin concentration clearly
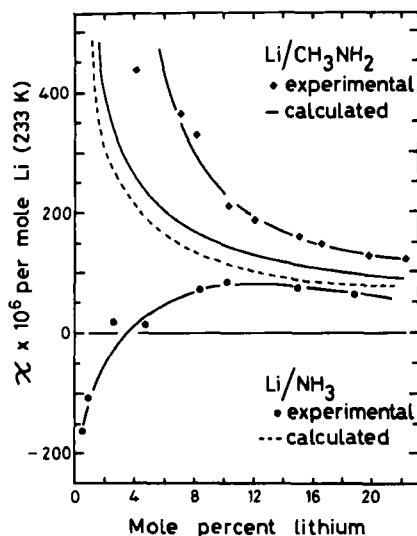

FIG. 27. The magnetic susceptibility of solutions of lithium in ammonia and in methylamine. The broken and solid lines indicate the predicted concentration variations of the susceptibility, based on an electron-gas picture in which electron–electron correlations are neglected (157a, 157b).

mimics the analytical concentration of the metal over a wide concentration range. This contrasts markedly with the situation at $-33°C$ and $0°C$ (Fig. 5).

Detailed magnetic susceptibility studies of both fluid and frozen solutions of lithium in methylamine have now been carried out (*157a,* *157b*). The data for lithium–methylamine solutions at $-40°C$ are shown in Fig. 27. The corresponding behavior of lithium–ammonia solutions is also shown. The observed susceptibility of lithium–methylamine solutions is in reasonable agreement with the calculated susceptibility of a free-electron gas (neglecting electron-correlation effects). In contrast, large diamagnetic deviations are observed for lithium–ammonia solutions below ~ 8 MPM (see Section III,A,2). Clearly, the methylamine solutions do not display the extensive spin-pairing phenomena observed in ammonia solutions at $-40°C$. The electronic properties of the corresponding solid expanded-metal compounds, including lithium 2,1,1-cryptate electride were discussed in the recent ACS symposium (*157b*) (see also Ref. *113a*).

REFERENCES

1. Banerjee, A., and Simons, J., *J. Chem. Phys.* **68**, 415 (1978).
2. Bar-Eli, K., and Tuttle, T. R., Jr., *Bull. Am. Phys. Soc.* [2] **8**, 352 (1963).
3. Bar-Eli, K., and Tuttle, T. R., Jr., *J. Chem. Phys.* **40**, 2508 (1964); **44**, 114 (1966).
4. Becker, E., Lindquist, R. H., and Alder, B. J., *J. Chem. Phys.* **25**, 971 (1956).
5. Bethe, H., *in* "Solid State Physics" (J. S. Blakemore, ed.), Saunders, Philadelphia, Pennsylvania, 1970.
6. Beuneu, F., and Monod, P., *Phys. Rev. B: Condens. Matter* **18**, 2422 (1978).
7. Boag, J. W., and Hart, E. J., *Nature (London)* **197**, 45 (1963).
8. Breitschwerdt, K. G., and Radscheit, H., *Ber. Bunsenges. Phys. Chem.* **80**, 797 (1976).
9. Brodsky, A. M., and Tsarevsky, A. V., *Adv. Chem. Phys.* **44**, 483 (1980).
10. Buntaine, J. R., Ph.D. Thesis, Cornell University, Ithaca, New York (1980), on file with University Microfilms, Order No. 8015643.
11. Buntaine, J. R., Sienko, M. J., and Edwards, P. P., *J. Phys. Chem.* **84**, 1230 (1980).

12. Carrington, A., and McLachlan, A. D., "Introduction to Magnetic Resonance." Harper & Row, New York, 1967.
13. Catterall, R., *in* "Metal-Ammonia Solutions" (J. J. Lagowski and M. J. Sienko, eds.), p. 105. Butterworth, London, 1970.
14. Catterall, R., and Carmichael, I., comments at Colloque Weyl V, *J. Phys. Chem.* **84,** 1128 (1980).
15. Catterall, R., and Edwards, P. P., *Adv. Mol. Relaxation Processes* **7,** 87 (1975).
16. Catterall, R., and Edwards, P. P., *Adv. Mol. Relaxation Interaction Processes* **13,** 123 (1978).
17. Catterall, R., and Edwards, P. P., *Adv. Mol. Relaxation Interaction Processes* (in press).
18. Catterall, R., and Edwards, P. P., *Chem. Phys. Lett.* **42,** 540 (1976).
19. Catterall, R., and Edwards, P. P., *Chem. Phys. Letts.* **43,** 122 (1976).
20. Catterall, R., and Edwards, P. P., *J. Chem. Soc., Chem. Commun.* p. 591 (1980).
21. Catterall, R., and Edwards, P. P., *J. Phys. Chem.* **79,** 3010 (1975).
22. Catterall, R., and Edwards, P. P., *J. Phys. Chem.* **84,** 1196 (1980).
23. Catterall, R., and Edwards, P. P., *Mol. Phys.* **32,** 555 (1976).
24. Catterall, R., and Edwards, P. P., *Solid State Commun.* (in press).
25. Catterall, R., and Edwards, P. P., *Int. Symp. Magn. Reson., 6th, 1977* p. 89 (1977).
26. Catterall, R., Edwards, P. P., Slater, J., and Symons, M. C. R., *Chem. Phys. Lett.* **64,** 275 (1979).
27. Catterall, R., and Mott, N. F., *Adv. Phys.* **18,** 665 (1969).
28. Catterall, R., Slater, J., Seddon, W. A., and Fletcher, J. W., *Can. J. Chem.* **54,** 3110 (1976).
29. Catterall, R., and Symons, M. C. R., *J. Chem. Soc.* p. 13 (1966).
30. Catterall, R., Symons, M. C. R., and Tipping, J. W., *J. Chem. Soc.* p. 1529 (1966); p. 1234 (1967).
31. Chan, S. I., Austin, J. A., and Paez, O. A., *in* "Metal-Ammonia Solutions" (J. J. Lagowski and M. J. Sienko, eds.), p. 425. Butterworth, London, 1970.
32. Chen, K. S., Mao, S. W., Nakamura, K., and Hirota, N., *J. Am. Chem. Soc.* **93,** 6004 (1971).
33. Chieux, P., and Sienko, M. J., *J. Chem. Phys.* **53,** 566 (1970).
34. Cohen, M. H., *Rev. Mod. Phys.* **40,** 839 (1968).
35. Cohen, M. H., and Jortner, J., *J. Phys. Chem.* **79,** 2900 (1975).
36. Cohen, M. H., and Jortner, J., *Phys. Rev. B: Solid State* **13,** 1548 (1976).
37. Cohen, M. H., and Thompson, J. C., *Adv. Phys.* **17,** 857 (1968).
38. Colloque Weyl IV. Electrons in fluids—the nature of metal-ammonia solutions, *J. Phys. Chem.* **79,** No. 26 (1975).
39. Colloque Weyl V. Excess electrons and metal-ammonia solutions, *J. Phys. Chem.* **84,** 1065 (1980).
40. Copeland, D. A., Kestner, N. R., and Jortner, J. J., *J. Chem. Phys.* **53,** 1189 (1970).
41. Cusack, N. E., *Proc. Scott. Univ. Summer Sch. Phys.* **19,** 455 (1978).
42. DaGue, M. G., Landers, J. S., Lewis, H. L., and Dye, J. L., *Chem. Phys. Lett.* **66,** 169 (1979).
43. Dalton, L. R., Rynbrandt, J. D., Hansen, E. M., and Dye, J. L., *J. Chem. Phys.* **44,** 3969 (1966).
44. Damay, P., and Chieux, P., *J. Phys. Chem.* **84,** 1203 (1980).
45. Davis, H. T., and Brown, R. G., *Adv. Chem. Phys.* **31,** 329 (1975).
46. Davy, H., *Philos. Trans. R. Soc. London* **98,** 1 (1808).
47. Demortier, A., Ph.D. Thesis, Lille (1970).

48. Dorfman, L. M., and Jou, F. Y., *in* "Electrons in Fluids" (J. Jortner and N. R. Kestner, eds.), p. 447. Springer-Verlag, Berlin and New York, 1973.
49. Douthit, R. C., and Dye, J. L., *J. Am. Chem. Soc.* **82,** 4472 (1960).
50. Dukel'skii, V. M., Zandberg, E. Ya., and Ionov, N. I., *Dokl. Akad. Nauk. SSSR,* **62,** 232 (1948), cited by J. L. Dye, in Ref. *51.*
51. Dye, J. L., *Angew. Chem., Int. Ed. Engl.* **18,** 587 (1979).
52. Dye, J. L., *Prog. Macrocyclic Chem.* **1,** 63 (1979).
53. Dye, J. L., *Pure Appl. Chem.* **49,** 3 (1977).
54. Dye, J. L., *in* "Metal-Ammonia Solutions" (J. J. Lagowski and M. J. Sienko, eds.), p. 1. Butterworth, London, 1970.
55. Dye, J. L., *in* "Electrons in Fluids" (J. Jortner and N. R. Kestner, eds.), p. 77. Springer-Verlag, Berlin and New York, 1973.
55a. Dye, J. L., *Sci. American* **237**(7), 92 (1977).
56. Dye, J. L., Andrews, C. W., and Ceraso, J. M., *J. Phys. Chem.* **79,** 3076 (1975).
57. Dye, J. L., Ceraso, J. M., Lok, M. T., Barnett, B. L., and Tehan, F. J., *J. Am. Chem. Soc.* **96,** 608 (1974).
58. Dye, J. L., and Dalton, L. R., *J. Phys. Chem.* **71,** 184 (1967).
59. Edwards, P. P., *J. Chem. Phys.* **70,** 2631 (1979).
60. Edwards, P. P., *J. Phys. Chem.* **84,** 1215 (1980).
61. Edwards, P. P., *Chem. Rev.* (to be submitted for publication).
62. Edwards, P. P., *Phys. Chem. Liq.* **10,** 189 (1981).
63. Edwards, P. P., Buntaine, J. R., and Sienko, M. J., *Phys. Rev. B: Condens. Matter* **19,** 5835 (1979).
64. Edwards, P. P., and Catterall, R., *Can. J. Chem.* **55,** 2258 (1977).
65. Edwards, P. P., and Catterall, R., *Philos. Mag. [Part] B* **39,** 81, 371 (1979).
65a. Edwards, P. P., Guy, S. C., Holton, D. M., and McFarlane, W., *J. Chem. Soc., Chem. Commun.* p. 1185 (1981).
66. Edwards, P. P., Lusis, A. R., and Sienko, M. J., *J. Chem. Phys.* **72,** 3103 (1980).
67. Edwards, P. P., and Schroer, W., unpublished work.
68. Edwards, P. P., and Sienko, M. J., *Phys. Rev. B: Solid State* **17,** 2575 (1978).
69. Edwards, P. P., and Sienko, M. J., *J. Am. Chem. Soc.* **103,** 2967 (1981).
70. Edwards, P. P., and Sienko, M. J., *Acc. Chem. Research* **15,** 87 (1982).
71. Elliott, R. J., *Phys. Rev.* **96,** 266 (1954).
72. Essig, W., Ph.D. Dissertation, University of Karlsruhe (1978), cited by Schindewolf (*148*).
73. Even, U., Swennumson, R. D., and Thompson, J. C., *Can. J. Chem.* **55,** 2240 (1977).
74. Feng, Da-Fei, and Kevan, L., *Chem. Rev.* **80,** 1 (1980).
75. Fletcher, J. W., and Seddon, W. A., *J. Phys. Chem.* **79,** 3055 (1975).
76. Freed, S., and Sugarman, N., *J. Chem. Phys.* **11,** 354 (1943).
77. Freyland, W., *J. Non-Cryst. Solids* **35/36,** 1313 (1980).
78. Friedman, L. R., and Tunstall, D. P., eds., "The Metal Non-Metal Transition in Disordered Systems." Scottish Universities Summer School in Physics, Edinburgh University, Edinburgh, 1978.
79. Fullmer, J. Z., "Sir Humphry Davy's Published Works." Harvard Univ. Press, Cambridge, Massachusetts.
80. Gibson, G. E., and Argo, W. L., *J. Am. Chem. Soc.* **40,** 1327 (1918).
81. Glasstone, S., "Textbook of Physical Chemistry." Van Nostrand-Reinhold, Princeton, New Jersey, 1940.
82. Glaunsinger, W. S., *J. Phys. Chem.* **84,** 1163 (1980).
83. Glaunsinger, W. S., White, T. R., von Dreele, R. B., Gordon, D. A., Marzke, R. F., Bowman, A. L., and Yarnell, J. L., *Nature (London)* **271,** 414 (1978).

84. Gold, M., and Jolly, W. L., *Inorg. Chem.* **1**, 818 (1962).
85. Gold, M., Jolly, W. L., and Pitzer, K. S., *J. Am. Chem. Soc.* **84**, 2264 (1962).
86. Goodenough, J. B., *in* "New Developments in Semiconductors" (R. R. Wallace, R. Hams, and M. J. Zuckermann, eds.), p. 107. Nordhoff Int., Gröningen, Leyden, 1971.
87. Goodenough, J. B., *in* "The Robert A. Welch Foundation Conferences on Chemical Research, XIV. Solid State Chemistry," Chapter 3. Houston, Texas, 1970. This article outlines similar considerations for narrow d-band materials.
88. Harris, R. L., Ph.D. Thesis, University of Texas at Austin (1979).
88a. Harris, R. L., and Lagowski, J. J., *J. Phys. Chem.* **85**, 856 (1981).
89. Hart, E. J., ed., "Solvated Electron," American Chemical Society, Washington, D.C., 1965.
90. Hart, E. J., and Boag, J. W., *J. Am. Chem. Soc.* **84**, 4090 (1963).
91. Hensel, F., *Ber. Bunsenges. Phys. Chem.* **80**, 786 (1976).
92. Hensel, F., *Can. J. Chem.* **55**, 2225 (1977).
93. Herzfeld, K. F., *Phys. Rev.* **29**, 701 (1927).
94. Hirasawa, M., Nakamura, Y., and Shimoji, M., *Ber. Bunsenges. Phys. Chem.* **82**, 815 (1978).
95. Hirota, N., and Kreilick, R., *J. Am. Chem. Soc.* **88**, 614 (1966).
96. Holcomb, D. F., *Proc. Scott. Univ. Summer Sch. Phys.* **19**, 251 (1978).
97. Huster, E., *Ann. Phys. (Leipzig)* [5] **33**, 477 (1938).
98. Hutchison, C. A., and Pastor, R. C., *J. Chem. Phys.* **21**, 1959 (1953).
99. International Conference on Electrons in Fluids, Banff, Alberta, Canada, 1976, *Can. J. Chem.* **55**, 1796 (1977).
100. Jen, C. K., Bowers, V. A., Cochran, E. L., and Foner, S. N., *Phys. Rev.* **126**, 1749 (1962).
101. Jortner, J., *J. Chem. Phys.* **30**, 839 (1959).
102. Jortner, J., *Ber. Bunsenges. Phys. Chem.* **75**, 696 (1971).
103. Jortner, J., and Kestner, N. R., eds., "Electrons in Fluids," Colloque Weyl III. Springer-Verlag, Berlin and New York, 1973.
104. Jortner, J., Rice, S. A., and Wilson, E. G., *in* "Metal-Ammonia Solutions" (G. Lepoutre and M. J. Sienko, eds.), p. 222. Benjamin, New York, 1964.
105. Kestner, N. R., *in* "Electrons in Fluids" (J. Jortner and N. R. Kestner, eds.), p. 1. Springer-Verlag, Berlin and New York, 1973.
106. Knox, R. S., "Theory of Excitons." Academic Press, New York, 1963.
107. Koehler, W. H., and Lagowski, J. J., *J. Phys. Chem.* **73**, 2329 (1969).
108. Kohn, W., *Solid State Phys.* **5**, 258 (1957).
109. Kraus, C. A., *J. Am. Chem. Soc.* **29**, 1557 (1907).
110. Kraus, C. A., *J. Am. Chem. Soc.* **30**, 1323 (1908).
111. Kraus, C. A., *J. Am. Chem. Soc.* **43**, 749 (1921); see also *J. Chem. Educ.* **30**, 83 (1953).
112. Krumhansl, J. A., *in* "Physics of Solids at High Pressures" (C. T. Tomizuka and R. M. Emrick, eds.), p. 425. Academic Press, New York, 1965.
113. Lagowski, J. J., and Sienko, M. J., eds., "Metal-Ammonia Solutions," Colloq. Weyl II, IUPAC. Butterworth, London, 1970.
113a. Landers, J. S., Dye, J. L., Stacy, A. M., and Sienko, M. J., *J. Phys. Chem.* **85**, 1096 (1981).
114. Lelieur, J. P., Ph.D. Thesis, Orsay (1972).
115. Lelieur, J. P., and Rigny, P., *J. Chem. Phys.* **59**, 1142 (1973).
116. Lepoutre, G., and Sienko, M. J., eds., "Metal-Ammonia Solutions," Colloq. Weyl I. Benjamin, New York, 1964.

117. Mahaffey, D. W., and Jerde, D. A., *Rev. Mod. Phys.* **40,** 710 (1968).
118. Mammano, N., *in* "Metal-Ammonia Solutions" (J. J. Lagowski and M. J. Sienko, eds.), p. 367. Butterworth, London, 1970.
119. Matalon, S., Golden, S., and Ottolenghi, M., *J. Phys. Chem.* **73,** 3098 (1969).
120. McHale, J., and Simons, J., *J. Chem. Phys.* **67,** 389 (1977).
121. Metcalf, H. J., *Nature (London)* **284,** 127 (1980).
122. Mott, N. F., *J. Phys. Chem.* **84,** 1199 (1980).
123. Mott, N. F., *J. Phys. Chem.* **79,** 2915 (1975).
124. Mott, N. F., "Metal-Insulator Transitions." Taylor & Francis, London, 1974.
125. Mott, N. F., *Philos. Mag.* [8] **6,** 287 (1961).
126. Mott, N. F., *Proc. Phys. Soc. London, Ser. A* **62,** 416 (1949).
127. Nakamura, Y., Horie, Y., and Shimoji, M., *J. Chem. Soc. Faraday Trans.* **70,** 1376 (1974).
128. Nakamura, Y., Toma, T., and Shimoji, M., *Phys. Lett. A* **60,** 373 (1977).
129. Nauta, H., and van Huis, C., *J. Chem. Soc., Faraday Trans.* **68,** 647 (1972).
130. Nicely, V. A., Breit-Rabi analysis of experimental values of L. R. Dalton. M.S. Thesis, Michigan State University (1966) (unpublished).
131. Normant, H., *Angew Chem., Int. Ed. Engl.* **6,** 1046 (1967).
132. Ogg, R. A., *J. Am. Chem. Soc.* **68,** 155 (1946); *J. Chem. Phys.* **14,** 114, 295 (1946); *Phys. Rev.* **69,** 243, 668 (1946).
133. Onsager, L., *Rev. Mod. Phys.* **40,** 709 (1968) (comments following the paper by J. C. Thompson, *ibid.* p. 704).
134. O'Reilly, D. E., *J. Chem. Phys.* **41,** 3729 (1964).
135. O'Reilly, D. E., and Tsang, T., *J. Chem. Phys.* **42,** 3333 (1965).
136. Paris, J. A., "The Life of Sir Humphry Davy." Henry Colburn and Richard Bentley, New Burlington Street, London, 1832.
137. Peer, W. J., and Lagowski, J. J., *J. Am. Chem. Soc.* **100,** 6260 (1978).
138. Peer, W. J., and Lagowski, J. J., *J. Phys. Chem.* **84,** 1110 (1980).
139. Phillips, C. S. G., and Williams, R. J. P., "Inorganic Chemistry." Oxford Univ. Press, London and New York, 1966.
140. Pikaev, A. K., "Solvated Electron in Radiation Chemistry." Nauka, Moscow, 1966.
141. Pitzer, K. S., *J. Am. Chem. Soc.* **80,** 5046 (1958).
142. Quinn, R. K., and Lagowski, J. J., *J. Phys. Chem.* **73,** 2326 (1969).
143. Reichardt, C., *in* "Solvent Effects in Organic Chemistry" (H. F. Ebel, ed.), Monogr. Mod. Chem. Ser., Verlag-Chemie, Weinheim, 1979 (for a wider discussion of the problem).
144. Rubinstein, G., Tuttle, T. R., and Golden, S., *J. Phys. Chem.* **77,** 2872 (1973).
145. Schettler, P. D., Jr., and Lepoutre, G., *J. Phys. Chem.* **79,** 2823 (1975).
146. Schindewolf, U., *Angew. Chem., Int. Ed. Engl.* **17,** 887 (1978).
147. Schindewolf, U., and Schulte-Frohlinde, D., *Ber. Bunsenges. Phys. Chem.,* **75,** 607 (1971).
148. Schindewolf, U., *Z. Phys. Chem. (Wiesbaden)* [N.F.] **112,** 153 (1978).
149. Schindewolf, U., and Werner, M., *J. Phys. Chem.* **84,** 1123 (1980).
150. Seddon, W. A., and Fletcher, J. W., *J. Phys. Chem.* **84,** 1104 (1980).
151. Seddon, W. A., Fletcher, J. W., and Catterall, R., *Can. J. Chem.* **55,** 2017 (1977).
152. Seddon, W. A., Fletcher, J. W., and Sopchyshyn, F. C., *Can. J. Chem.* **56,** 839 (1978).
153. Seddon, W. A., Fletcher, J. W., and Sopchyshyn, F. C., *Chem. Phys.* **15,** 377 (1976).
154. Sienko, M. J. *in* "Metal-Ammonia Solutions" (G. Lepoutre and M. J. Sienko, eds.), p. 23. Benjamin, New York, 1964.

155. Sienko, M. J., and Chieux, P., *in* "Metal-Ammonia Solutions" (J. J. Lagowski and M. J. Sienko, eds.) p. 339. Butterworth, London, 1970.
156. Slichter, C. P., "Principles of Magnetic Resonance." Harper & Row, New York, 1963.
157. Springett, B. E., Jortner, J., and Cohen, M. H., *J. Chem. Phys.* **48**, 2720 (1968).
157a. Stacy, A. M., Ph.D. Thesis, Cornell University, Ithaca, New York (1981).
157b. Stacy, A. M., Edwards, P. P., and Sienko, M. J., "ACS Symposium on Electronic Properties of Inorganic Solids, Las Vegas, March 1982," to be published *J. Solid State Chem.*
158. Steinberg, V., Voronel, A., Linsky, D., and Schindewolf, U., *Phys. Rev. Lett.* **45**, 1338 (1980).
159. Suchannek, R. G., Naiditch, S., and Kleijnot, O. J., *J. Appl. Phys.* **38**, 690 (1967).
160. Symons, M. C. R., *Chem. Soc. Rev.* p. 337 (1976).
161. Symons, M. C. R., *J. Phys. Chem.* **71**, 172 (1967).
162. Tehan, F. J., Barnett, B. L., and Dye, J. L., *J. Am. Chem. Soc.* **96**, 7203 (1974).
163. Teherani, T. H., Peer, W. J., Lagowski, J. J., and Bard, A. J., *J. Am. Chem. Soc.* **100**, 7768 (1978).
164. Thompson, J. C., "Electrons in Liquid Ammonia." Oxford Univ. Press (Clarendon), London and New York, 1976.
165. Thompson, J. C., *in* "The Chemistry of Non-Aqueous Solvents" (J. J. Lagowski, ed.), Vol. 2, p. 265. Academic Press, New York, 1967.
166. Toma, T., Nakamura, Y., and Shimoji, M., *Philos. Mag.* [8] **33**, 181 (1976).
167. von Dreele, R. B., Glaunsinger, W. S., Bowman, A. L., and Yarnell, J. L., *J. Phys. Chem.* **79**, 2992 (1975).
168. Vos, K. D., and Dye, J. L., *J. Chem. Phys.* **38**, 2033 (1963).
169. Warren, W. W., Jr., *Phys. Rev.* **3**, 3708 (1971).
170. Weber, S., Rice, S. A., and Jortner, J., *J. Chem. Phys.* **42**, 1907 (1965).
171. Webster, B., *J. Phys. Chem.* **84**, 1070 (1980).
172. Weyl, W., *Ann. Phys. (Leipzig)* **121**, 601 (1864).